8-22 Reflector Shroud and Radome BOR-MoM Analyses

BOR-MoM (Body of Revolution Method of Moments) analysis enables low runtime analyses of shrouds and axisymmetric radomes. A shroud, a drum-like structure extending from the main reflector, reduces the back- and side-lobes of a reflector which reduces crosstalk between closely spaced reflectors. Multiple point-to-point microwave links mounted on the same tower will interfere unless the back and side looking sidelobes are reduced. Although feeds can be designed to handle weather conditions, an alternative design uses a radome to protect the whole antenna. The radome can also reduce the tower wind loading of the reflector compared to the cuplike aspect of a paraboloid. The radome can also serve as the feed support and eliminate strut scatter. Of course, a normal BOR-MoM analysis cannot include strut but the analysis can provide a good guide to design.

The TICRA program CHAMP is used for these BOR-MoM analyses. The program designs axisymmetric feed horns by using optimization to determine dimensions. The basic design and analysis uses circular waveguide modal analysis that expands fields in each horn section and matches the modes in various sections at discontinuities. Accurate analyses add the currents excited on the exterior of the horn using BORMoM to produce correct results. The BORMoM portion of the program can be extended to include metal and dielectric bodies. We will add metallic reflectors and shrouds to perform these analyses. Additionally, layers of lossy dielectrics can be included to enable analyses of absorbers in shrouds and dielectric radomes. The thickness of the dielectric layers can be included in the optimization to produce better results.

8-22.1 Shrouds

We start with a prime focus single reflector. The CHAMP design of the horn locates the horn aperture at the *z*-axis center of the coordinates pointed along the positive *z*-axis which requires our positioning of the reflector. CHAMP accepts a radially symmetric reflector file (*.rsf format) used in the TICRA GRASP program. The attached command line window executable PARRSF generates this file and allows the reflector to be rotated and translated into position. CHAMP generates a pattern with its peak at 180° for this configuration (Figure 8-22.1). The first case uses a 50λ diameter reflector, f/D = 0.4, fed by a 10.3 dB gain axially corrugated horn (Section 7-3.3) with a 35° flare angle (Figure 8-22.1).

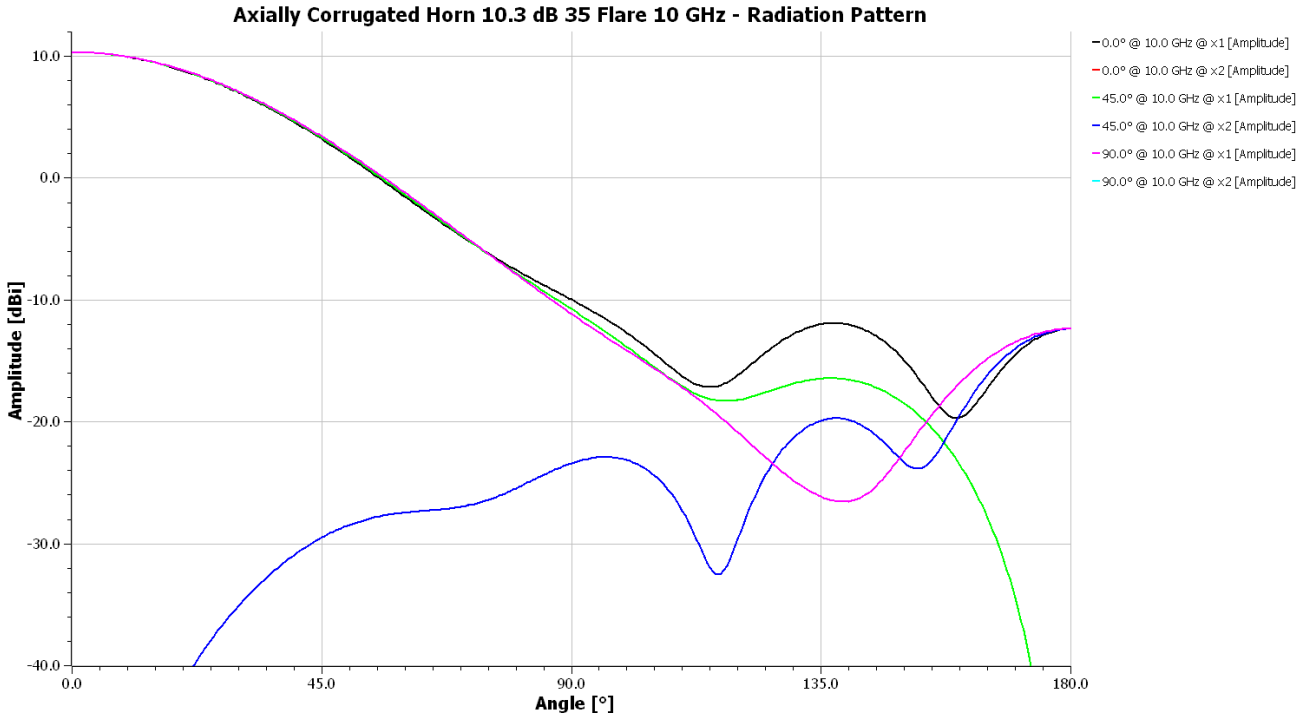

Figure 8-22.1 Feed pattern of Axially Corrugated Horn used for prime focus CHAMP reflector analysis

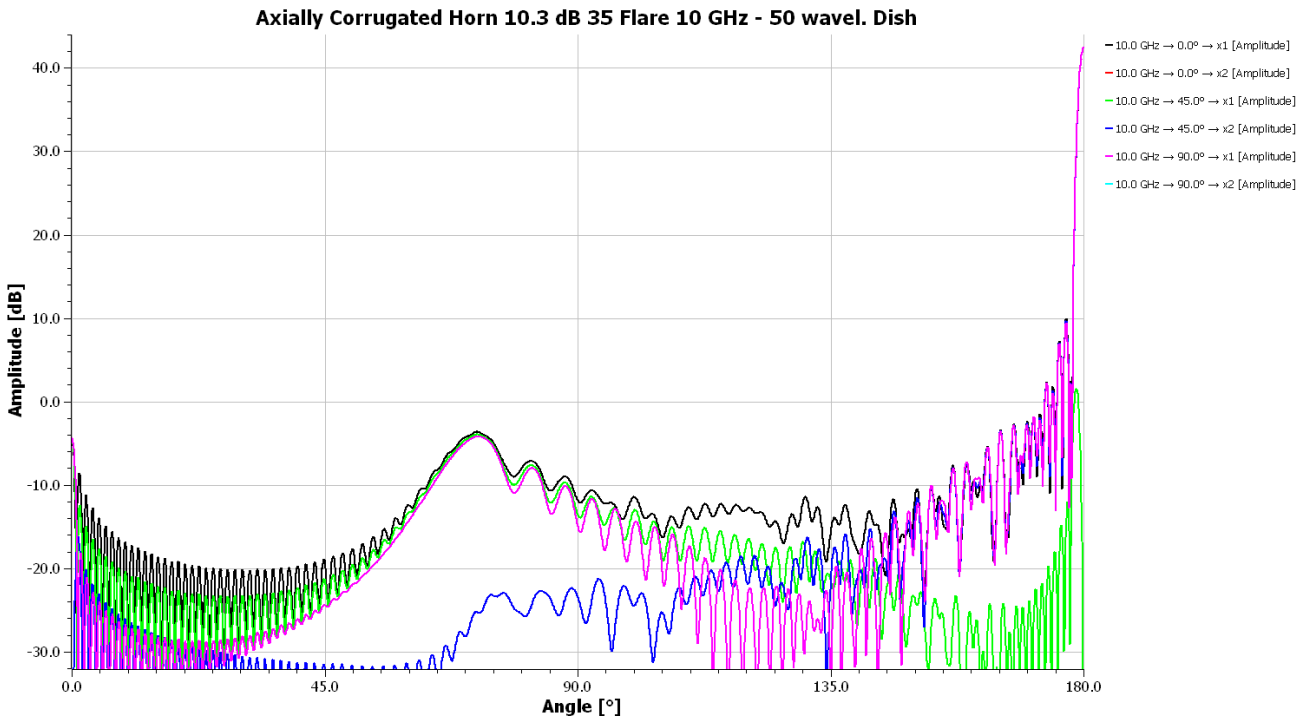

Figure 8-22.2 50λ diameter Single Reflector pattern from CHAMP

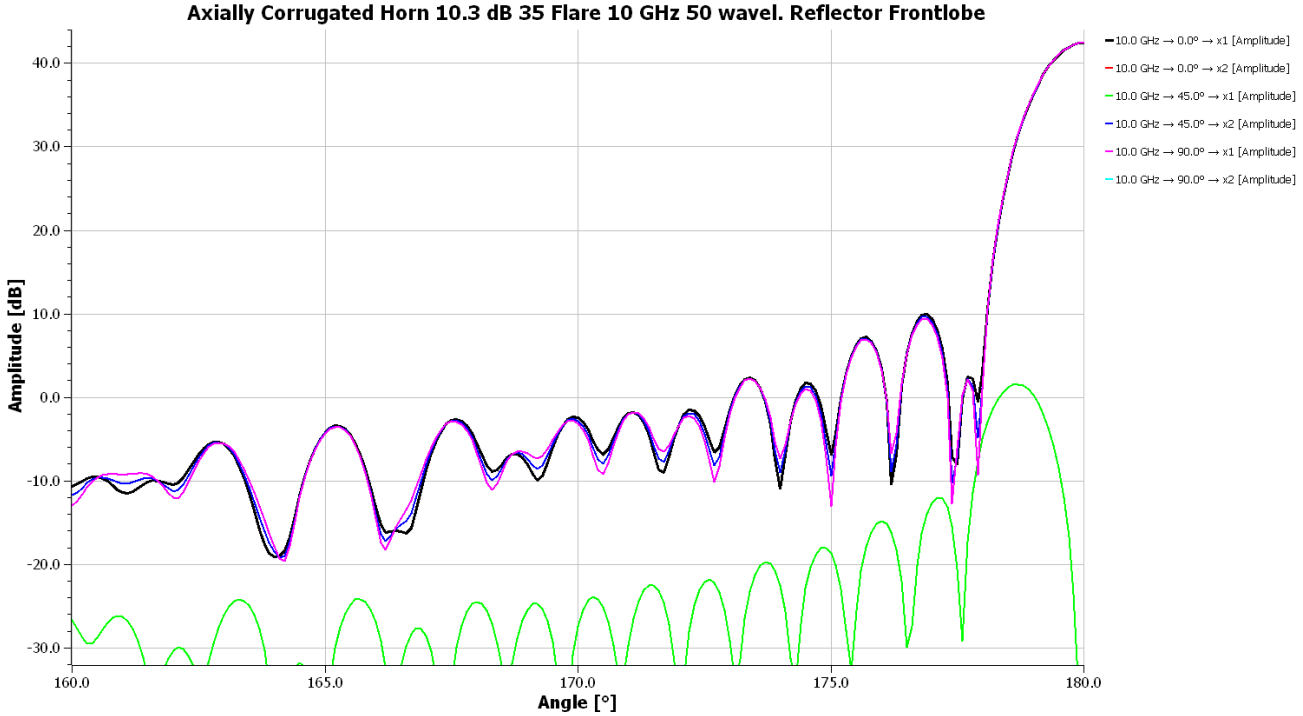

Figure 8-22.3 Front-lobe, beam peak, of 50λ diameter reflector in CHAMP analysis

Figures 8-22.2, 8-22.3, and 8-22.4 illustrate that the CHAMP analysis produces patterns with the peak at 180° and the back-lobe at 0°. The output *.cut file of the pattern from CHAMP can have its angles reversed and re-plotted to produce a beam peak at 0° if necessary. The peak front-lobe is 42.48 dBi while the back-lobe is -4.4 dBi producing a Front/Back (F/B) of 46.9 dB.

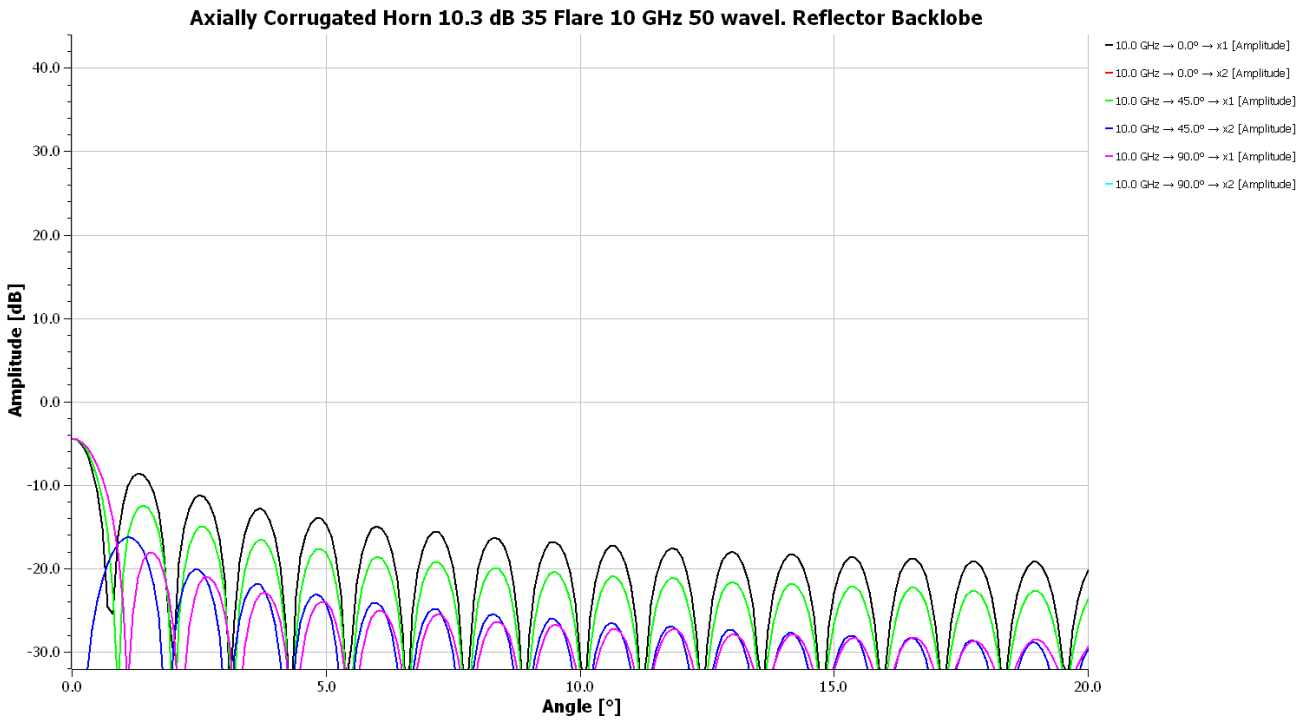

Figure 8-22.4 Back-lobe, beam peak, of 50λ diameter reflector in CHAMP analysis

The command line window executable program CHESHD generates an addition to the CHAMP geometry.tor file to include a metal (unlined) shroud to be attached to the edge of the reflector. The position of the edge of the reflector must be known. The shroud length and orientation angle become variables which can be used in a design optimization of CHAMP.

Modifications to CHAMP geometry.tor file

The reflector is added to the geometry.tor file that can be added using the "Create" horizontal tab in CHAMP which points to the *.rsp file.

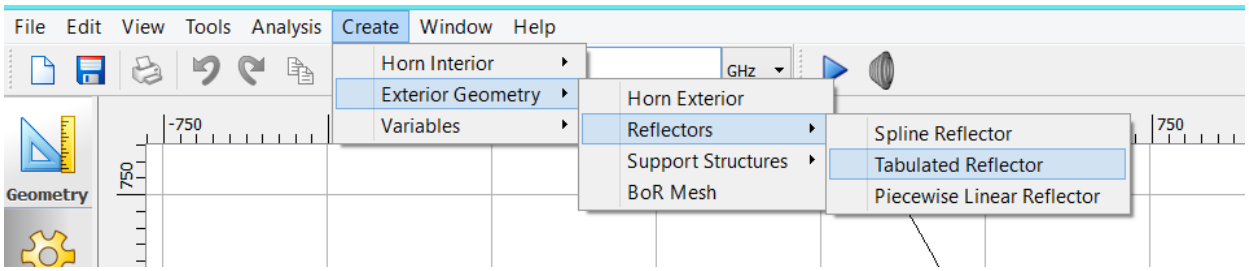

CHAMP adds the following to the geometry.tor file:

```
reflector  tabulated_circ_sym_reflector
(
  file_name        : ref50.rsf,
  r_unit           : mm,
  z_unit           : mm,
  z_offset         : 0.0 mm,
  obsolete_thickness : 0.0 mm
)
```

The name of the "tabulated_circ_sym_reflector is added to the list of scatterers at the top of geometry.tor:

```
horn  combined_horn_section
(
  horn_sections    : sequence(ref(circular_waveguide_section),ref(axial_section)),
  scatterers       : sequence(ref(horn_exterior),ref(reflector),ref(shroud_metal))
)
```

The program CHESHD generates the addition to the geometry.tor file for the metal shroud including the associated variables.

```
ZLOFF  real_variable
(
  value            : 0.0
)

DTR  real_variable
(
  value            : "atan(1.)/45."
)

SHANG  real_variable
(
  value            : 170.0
)

SHLEN  real_variable
(
  value            : 603.539319678652
)

SHCZ  real_variable
(
  value            : 365.62
)

SHCR  real_variable
(
  value            : 750.0
)

SHEZ  real_variable
(
  value            : "ref(SHCZ)+cos(ref(SHANG)*ref(DTR))*ref(SHLEN)"
)

SHER  real_variable
(
  value            : "ref(SHCR)+sin(ref(SHANG)*ref(DTR))*ref(SHLEN)"
)

shroud_metal  piecewise_linear_reflector
(
  z_offset         : "ref(ZLOFF)" mm,
  length_unit      : mm,
  nodes            : table
```

```
    (
    "ref(SHCZ)"  "ref(SHCR)"
    "ref(SHEZ)"  "ref(SHER)"
    )
)
```

SHLEN (shroud length) and SHANG (shroud angle, 180) variables can be used in a design optimization in CHAMP. The name of the "piecewise_linear_reflector" is added to the scatterer list at the top of the geometry.tor file.

```
  scatterers       : sequence(ref(horn_exterior),ref(reflector),ref(shroud_metal))
)
```

The altered geometry.tor is saved and CHAMP run with the addition of the metal shroud (20λ length).

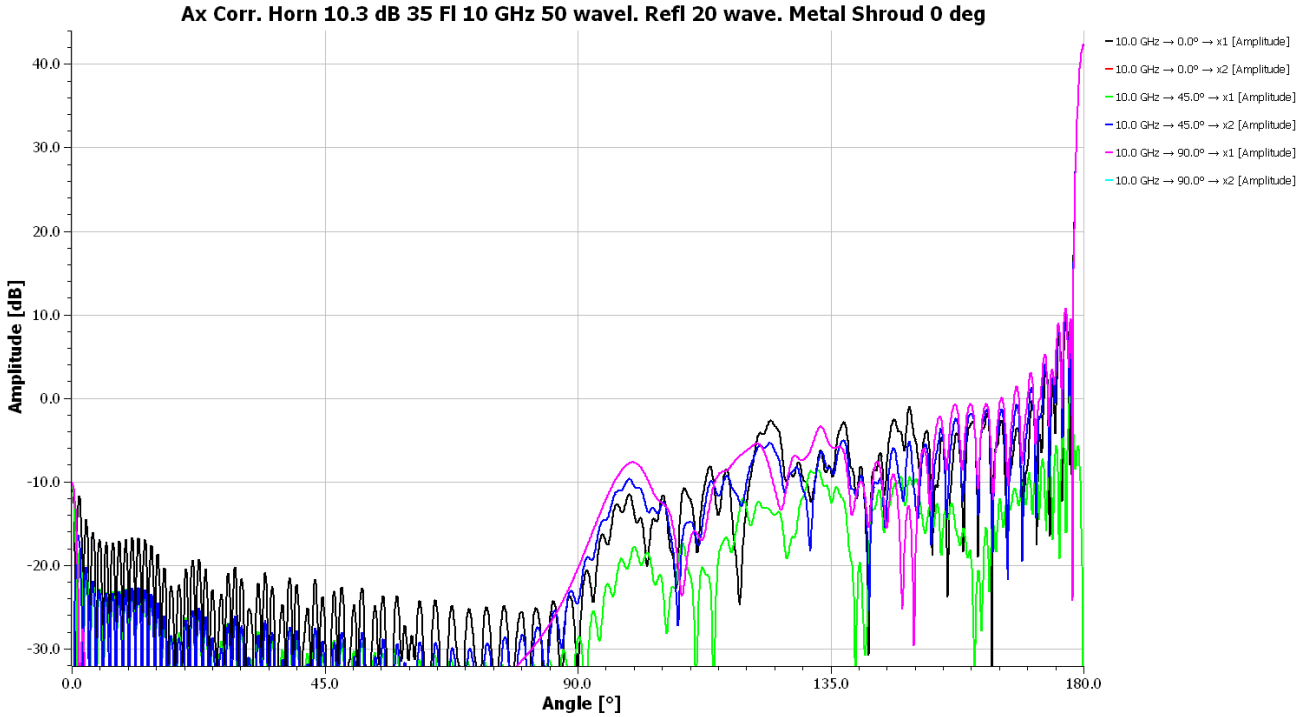

Figure 8-22.5 50λ reflector with 20λ long metal shroud with 0° (180°) cone

A comparison of Figure 8-22.2 and 8-22.5 shows that the metal shroud has reduced the spillover lobe significantly ~20 dB. Figure 8-22.6 illustrates that the peak gain and first few sidelobe levels have not changed from Figure 8-22.3. The backlobe at 0° has decreased about 6 dB when comparing Figure 8-22.7 with Figure 8-22.4

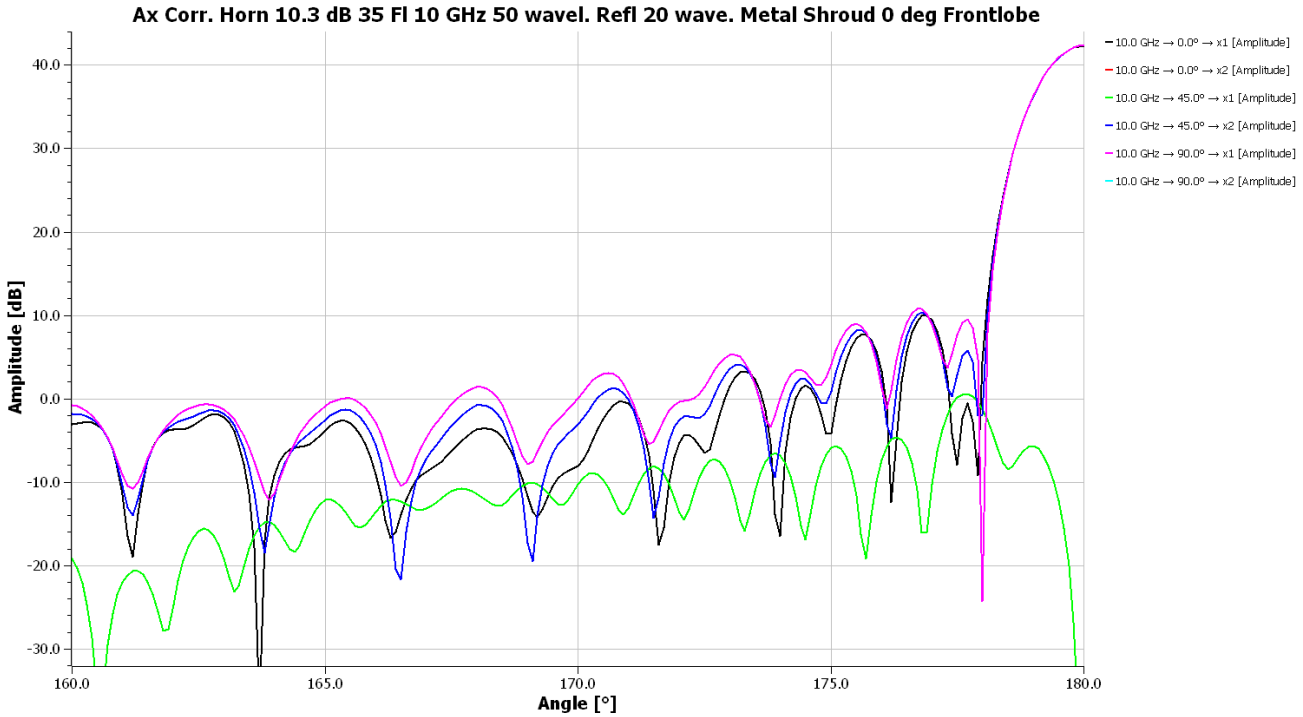

Figure 8-22.6 Front-lobe, beam peak, of 50λ diameter reflector w/ 20λ, 0° metal shroud in CHAMP analysis

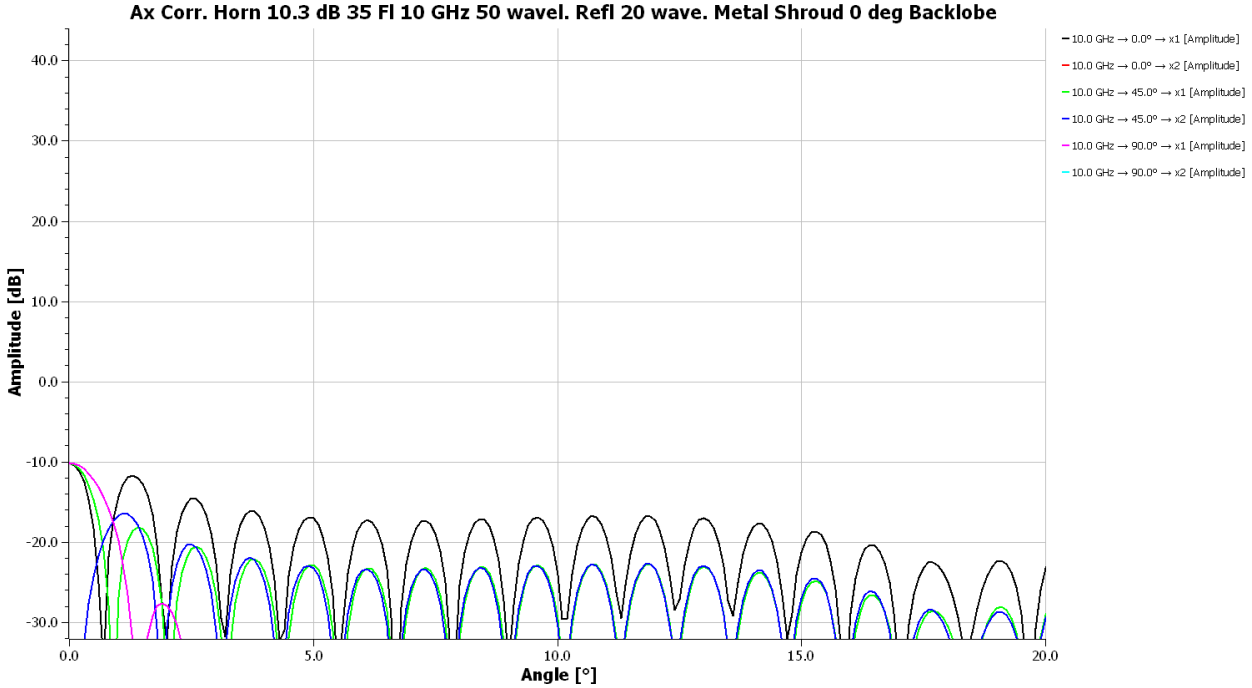

Figure 8-22.7 Back-lobe, beam peak, of 50λ diameter reflector w/ 20λ, 0° metal shroud in CHAMP analysis

The rotation of the metal shroud can be easily changed by altering SHANG in the geometry tab listing. Zero degree orientation to the shroud produces a large diameter waveguide and would set-up possible waveguide modes. Flaring the shroud (SHANG) by 5° (175°) outward changes the pattern. The peak gain (Figure 8-22.remains about the same and the spillover lobe is still reduced a similar amount, but the back lobe rises to about the same level (Figure 8-22.9) of the no shroud case (Figure 8-22.4)..

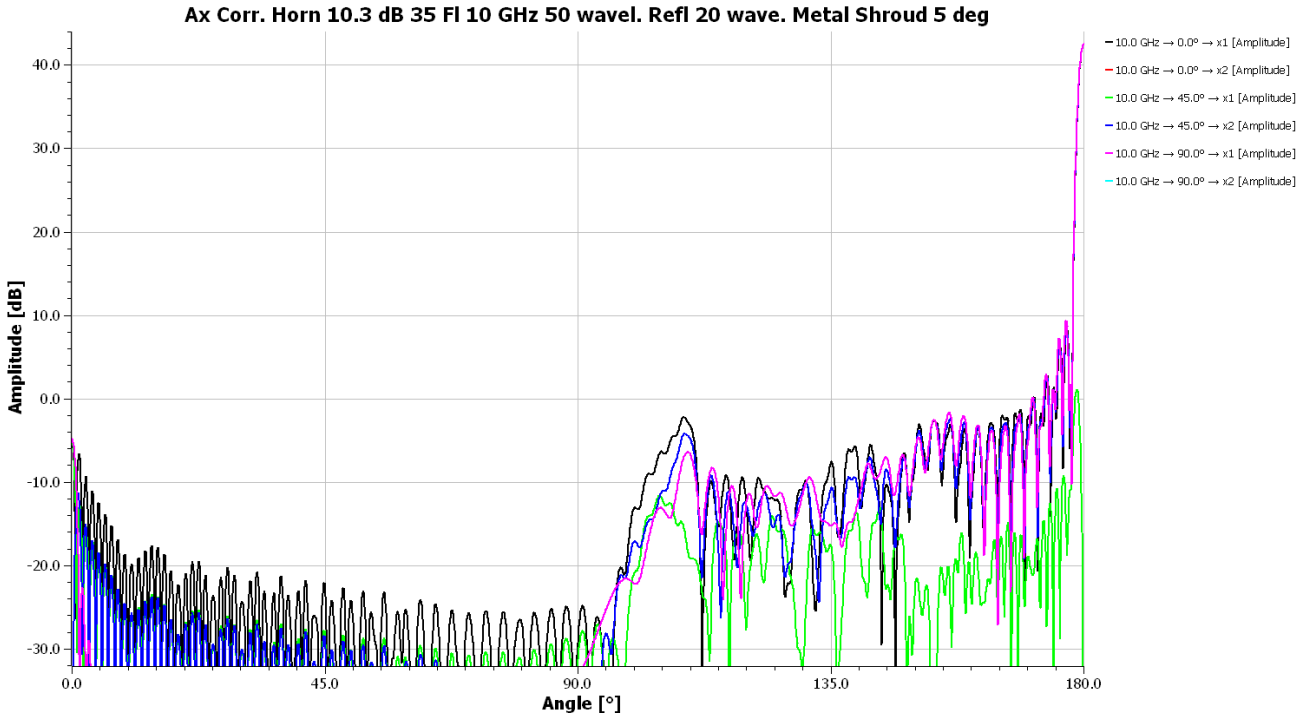

Figure 8-22.8 50λ reflector with 20λ long metal shroud with 5° (180°) cone

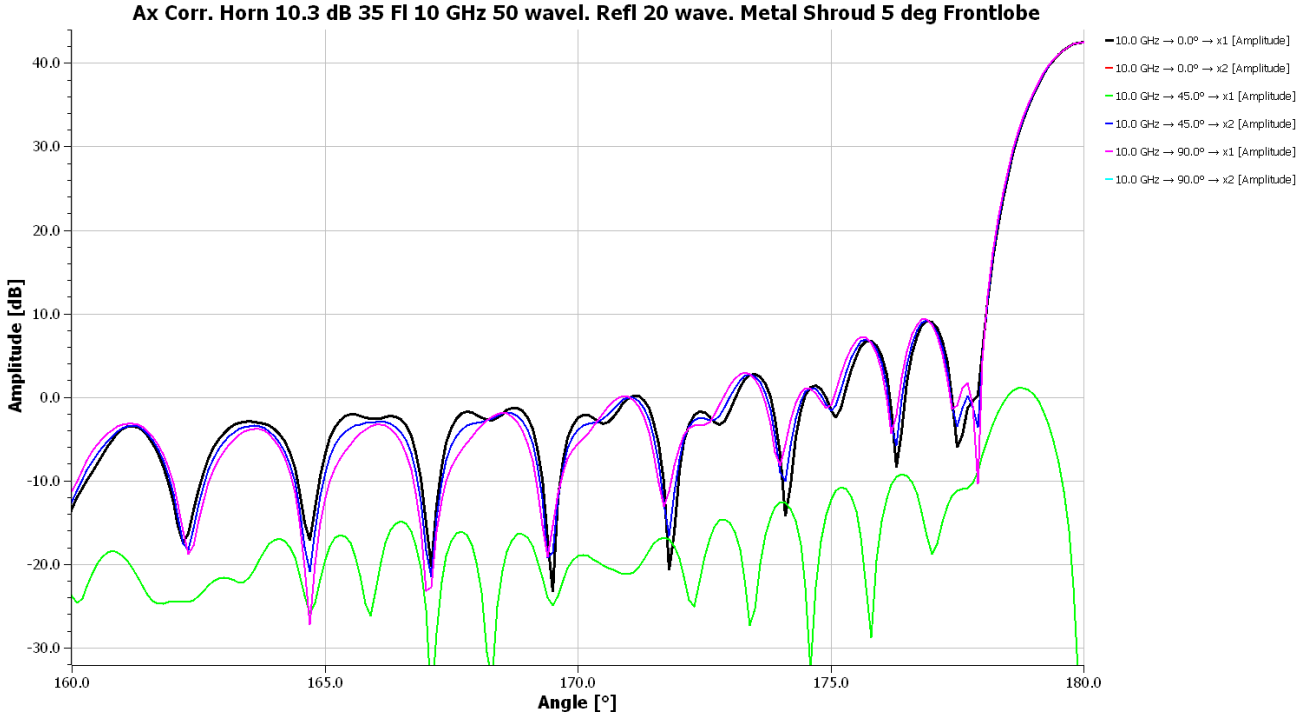

Figure 8-22.9 Front-lobe, beam peak, of 50λ diameter reflector w/ 20λ, 5° metal shroud in CHAMP analysis

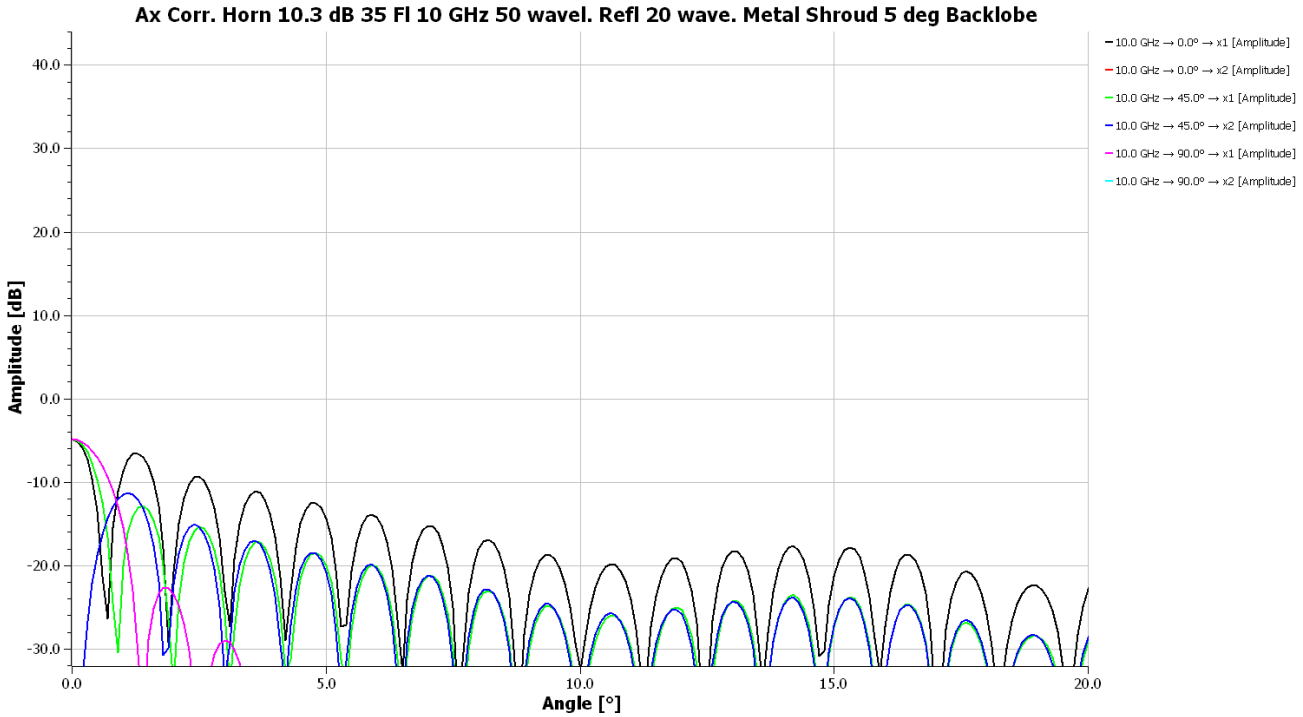

Figure 8-22.10 Back-lobe, beam peak, of 50λ diameter reflector w/ 20λ, 5° metal shroud in CHAMP analysis

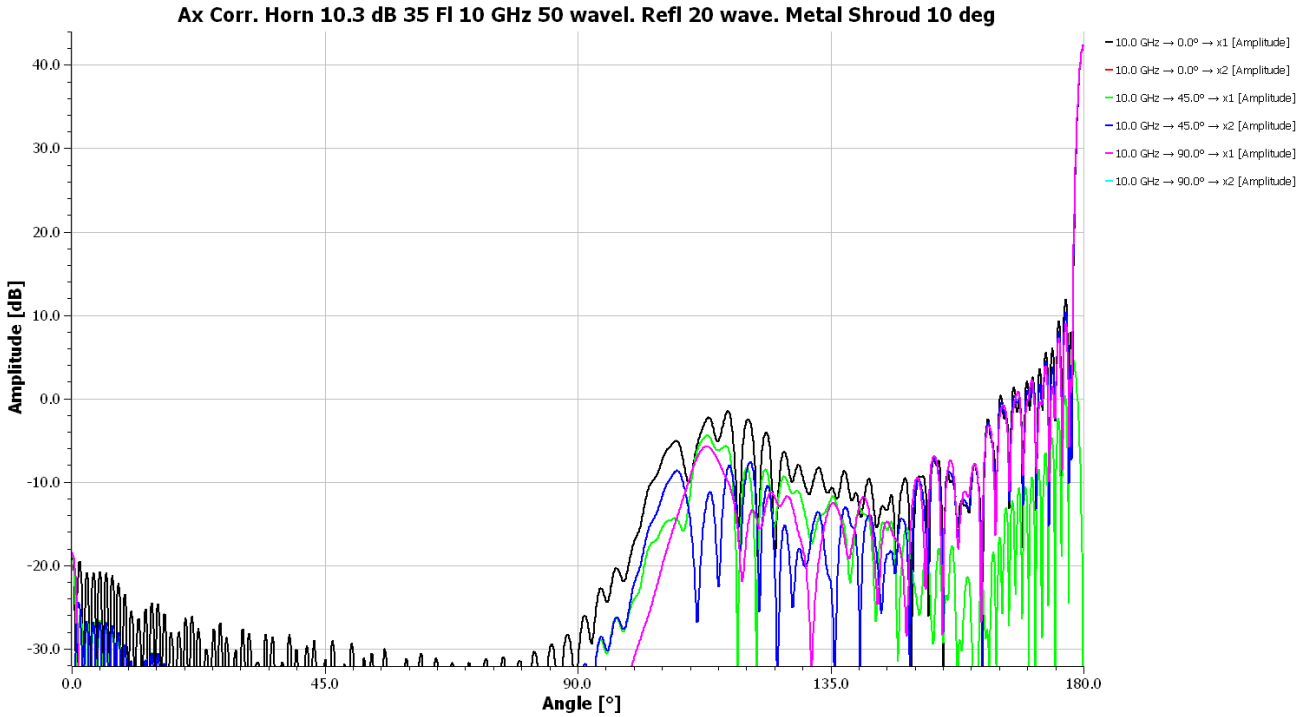

Figure 8-22.11 50λ diameter reflector with 20λ long metal shroud with 10° (170°) cone

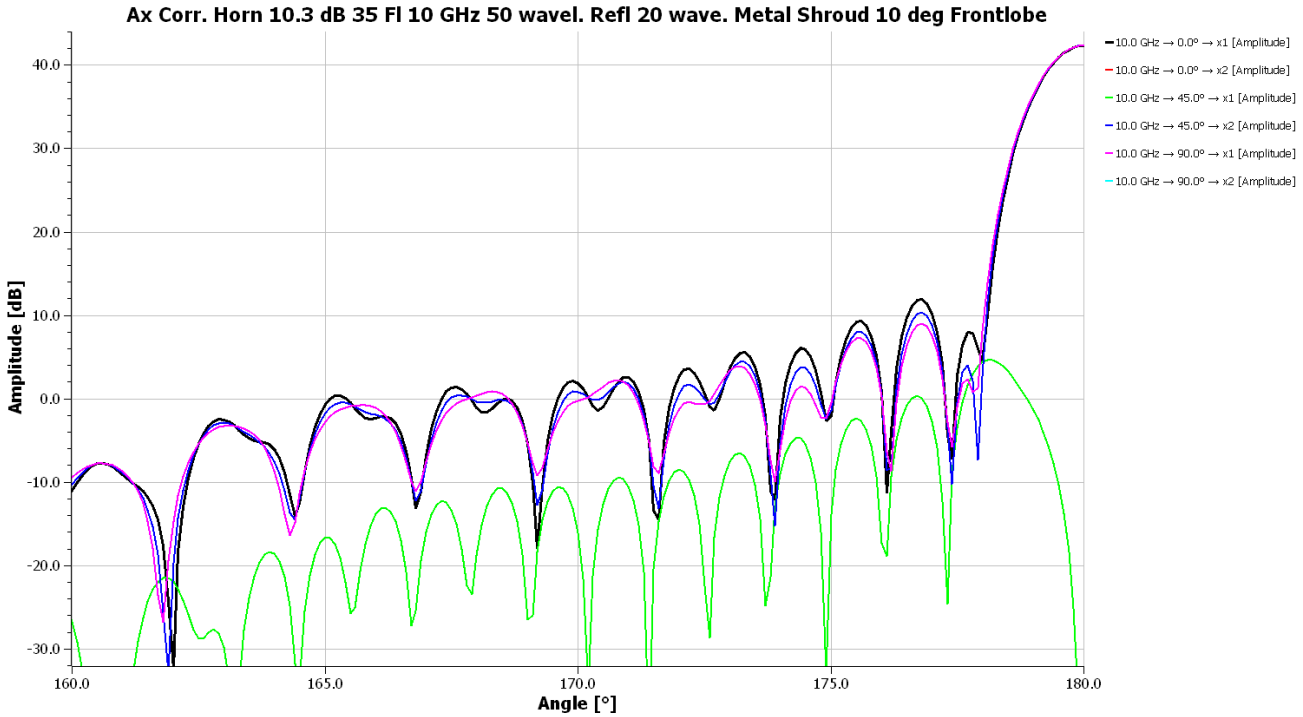

Figure 8-22.12 Front-lobe, beam peak, of 50λ diameter reflector w/ 20λ, 10° metal shroud in CHAMP analysis

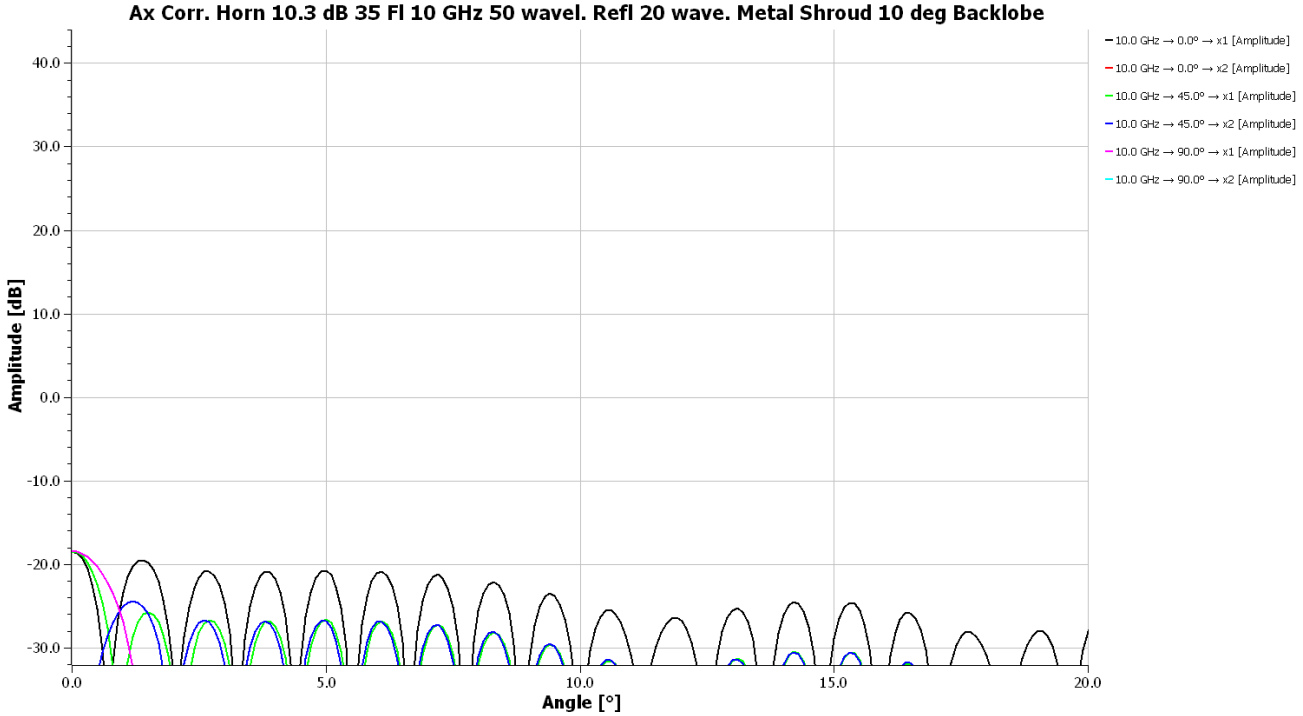

Figure 8-22.13 Back-lobe, beam peak, of 50λ diameter reflector w/ 20λ, 10° metal shroud in CHAMP analysis

Flaring the cone angle of the metal shroud to 10° has reduced both the spillover lobe (Figure 8-22.11 compared to Figure 8-22.5 or Figure 8-22.8) but has reduced the back lobe to -18 dBi. An optimization using the cone angle (SHANG) as its variable might produce better F/B and generally lower interring lobes.

The metal shroud reduces the spillover lobe which reduces the noise temperature contribution of radiation on soil and would improve G/T in a point-to-point microwave link. If we add absorber to the lining of the shroud, we expect a decrease in G/T as thermal radiation from the warm absorber adds noise.

Absorber Lined Prime Focus Reflector Shroud

Absorber lining the shroud reduces multiple reflections has the potential of reducing back and side radiation. The program CHASHD adds a single or multiple layer lossy dielectric (absorber) to the inside of the shroud.

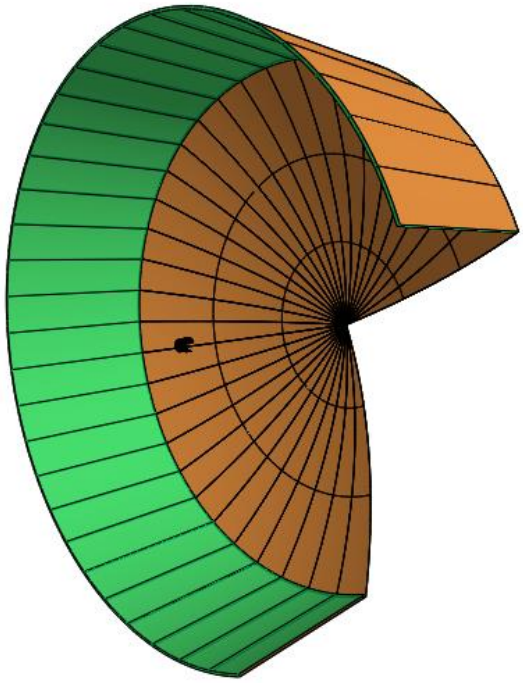

Figure 8-22.14 Absorber lined (lossy dielectric, green) layer added to shroud of prime focus reflector

The CHAMP geometry.tor addition is a bor_mesh object which allows dielectric layers.

```
SHTH1  real_variable
(
  value            : 6.993
)

TTS1  real_variable
(
  value            : "ref(SHTH1)"
)

DTR  real_variable
(
  value            : "atan(1.)/45."
)

SHANG  real_variable
(
  value            : 175.0
)
```

```
UVZS  real_variable
(
  value            : "cos(ref(SHANG)*ref(DTR))"
)

UVRS  real_variable
(
  value            : "sin(ref(SHANG)*ref(DTR))"
)

SHLEN  real_variable
(
  value            : 470.0
)

SHCZ  real_variable
(
  value            : 365.62
)

SHCR  real_variable
(
  value            : 750.0
)

SHEZ  real_variable
(
  value            : "ref(SHCZ)+ref(UVZS)*ref(SHLEN)"
)

SHER  real_variable
(
  value            : "ref(SHCR)+ref(UVRS)*ref(SHLEN)"
)

shroud_absorb  bor_mesh
(
  regions          : table
    (
        1    1.50000E+00    1.00000E+00    9.00000E-01
    ),
  nodes            : table
    (
        1  "ref(SHCZ)"  "ref(SHCR)"
        2  "ref(SHEZ)"  "ref(SHER)"
        3  "ref(SHCZ)-ref(UVRS)*ref(TTS1)"  "ref(SHCR)+ref(UVZS)*ref(TTS1)"
        4  "ref(SHEZ)-ref(UVRS)*ref(TTS1)"  "ref(SHER)+ref(UVZS)*ref(TTS1)"
    ),
  linear_segments  : table
    (
        1      1      2      0      1    0.00000E+00    0.00000E+00
        2      3      4      1      0   -1.00000E+00    0.00000E+00
        3      1      3      0      1   -1.00000E+00    0.00000E+00
        4      2      4      0      1   -1.00000E+00    0.00000E+00
```

```
    ),
  length_unit      : mm
)
```

The case illustrated has only one layer and a single lossy dielectric layer, while CHASHD allows input of multiple layers to the absorber. Because the absorber layers are thin, adding multiple thin layers increases runtime significantly compared to a single layer. A "bor_mesh" scatterer does not allow a *z_focus* offset of the "piecewise linear mesh" scatterer which means a simple offset cannot be used to account for the position of the phase center in the feed horn. The axially corrugated horn used in these examples has its phase center in the aperture plane. The thickness of a single layer absorber was adjusted to reduce reflection over a range of incidence angles.

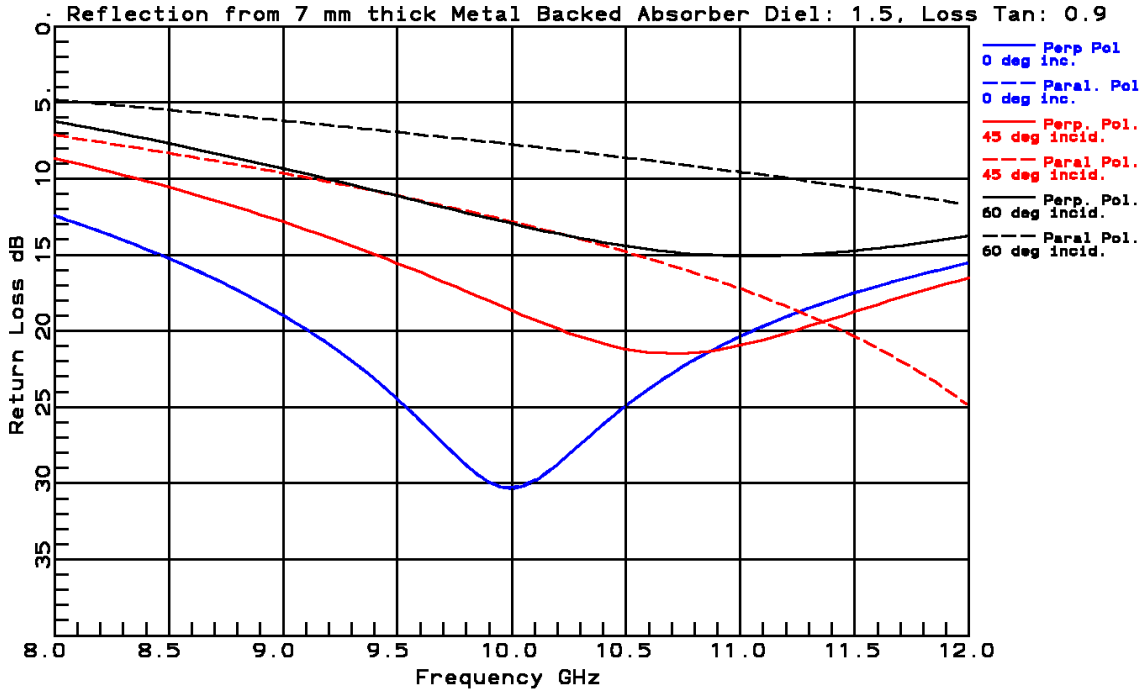

Figure 8-22.15 Single Layer Absorber Frequency Response (centered at 10 GHz)

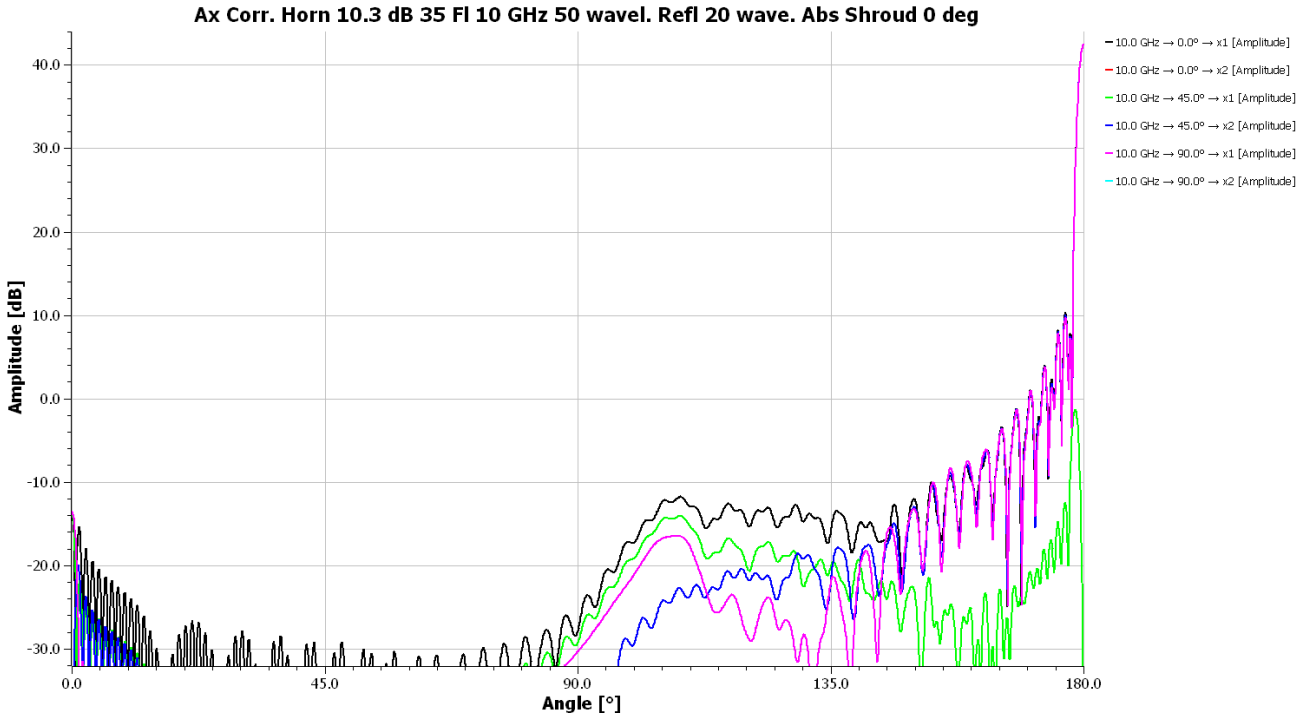

Figure 8-22.16 50λ reflector with 20λ long single layer absorber lined shroud with 0° (180°) cone

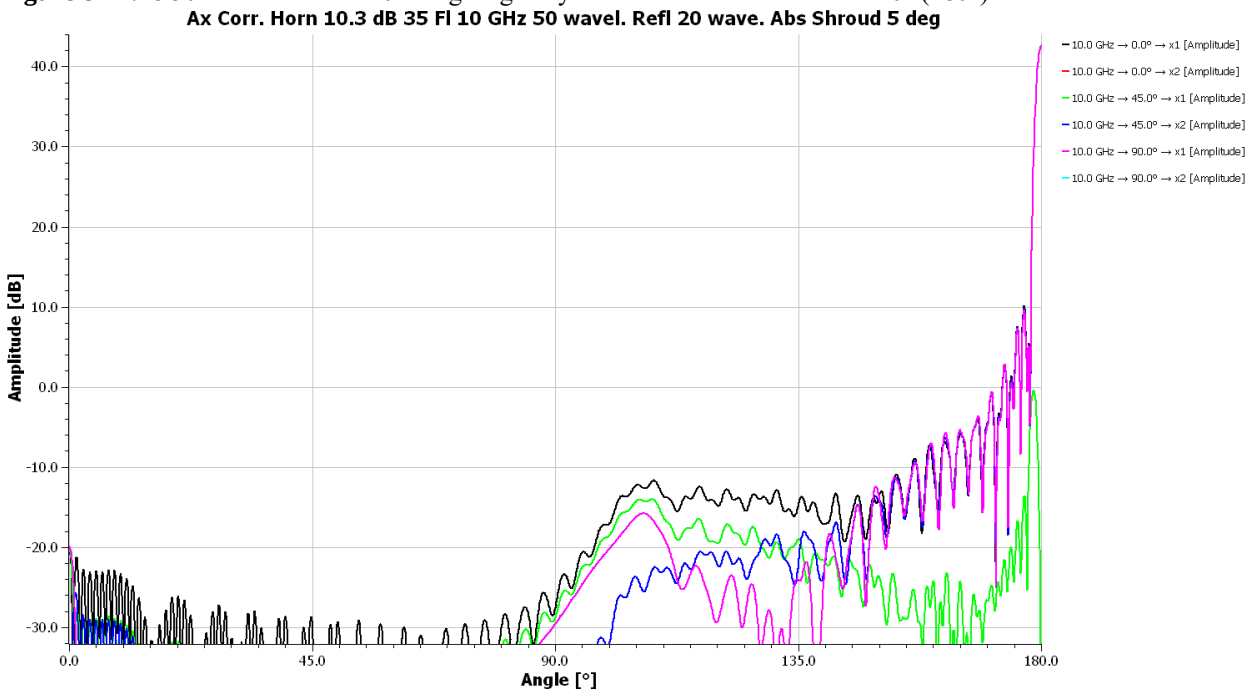

Figure 8-22.17 50λ reflector with 20λ long single layer absorber lined shroud with 5° (175°) cone

Figures 8-22.16 and 8-22.17 have similar patterns over most regions except for back radiation region where flaring the shroud into 5° cone reduces radiation levels.

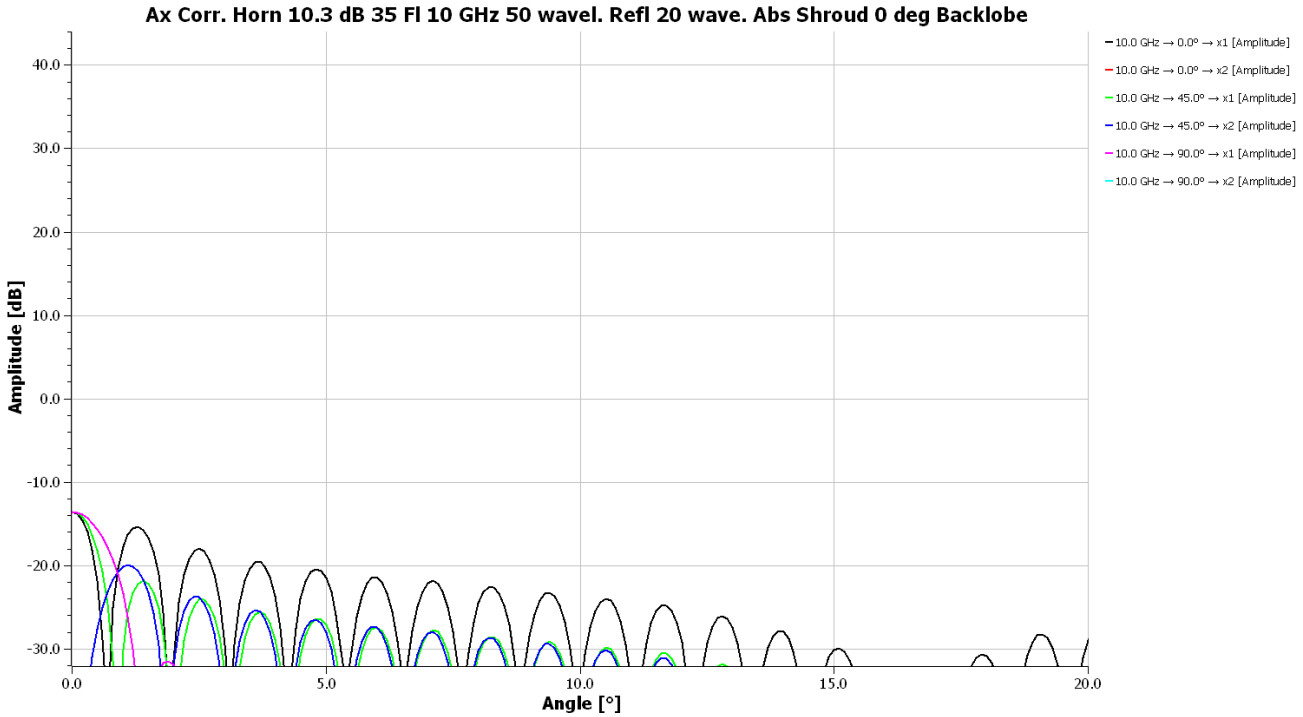

Figure 8-22.18 50λ reflector with 20λ long single layer absorber lined shroud with 0° (180°) cone back lobe

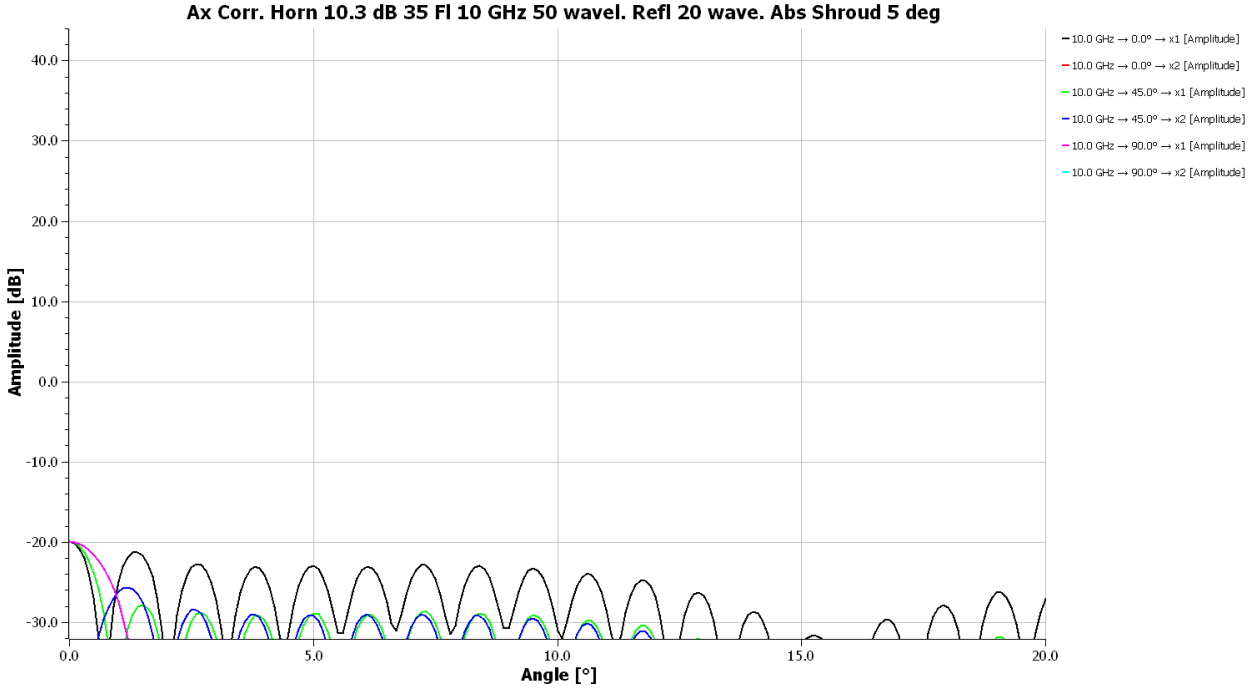

Figure 8-22.19 50λ reflector with 20λ long single layer absorber lined shroud with 5° (175°) cone back lobe

Flaring the single layer absorber lined shroud by 5° reduces the back radiation by about 6 dB and increasing F/B to 62 dB. Figures 8-22.17 and 8-22.18 show that lining the shroud with absorber reduces side radiation in the forward direct (30° to 90° off-boresight) compared to the metal shroud.

Cassegrain Reflector Analysis

We use the "create" tab in CHAMP to enter the tabulated rotationally symmetric reflector data that we can generate using the command window executable GRANETDS. GRANETDS enables specification of dual reflectors in the various parameters commonly used. The *,rsf files of both reflectors are shifted by the main vertex to feed distance to center the feed (phase center) at the origin. The examples given below use a 20 dB gain Potter horn to feed a 150λ diameter main reflector of a Cassegrain antenna using a 30λ diameter subreflector. Figure 8-22.20 plots the CHAMP central geometry.

BOR-MoM analysis includes the multiple interactions between the feed, subreflector, and main reflector which will be required in a PO/PTD analysis. Of course, a PO/PTD analysis converges rapidly when we use an iterative analysis to compute the effect of additional currents excited on the various surfaces. The mutual coupling between these scatterers is small and the effects are small. The BOR-MoM analysis must include the exterior of a horn feed antenna because the aperture currents of the modal analysis only interact once with exterior scatterers. The external horn currents are the blockage currents in the MoM analysis.

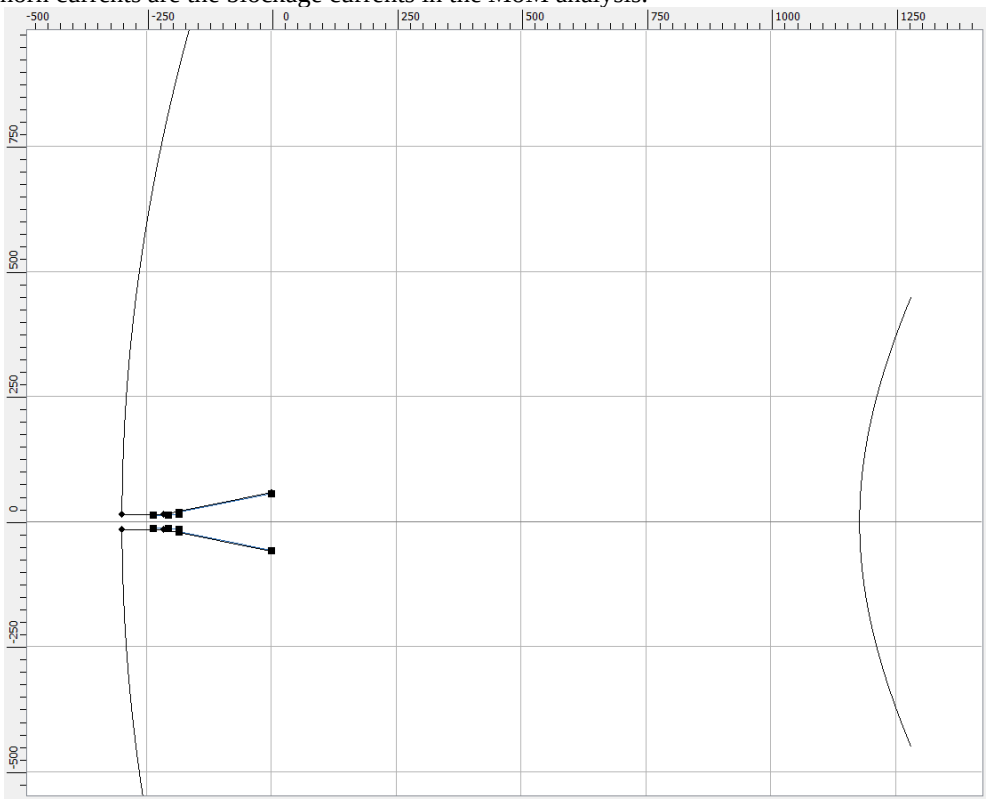

Figure 8-22.20 CHAMP geometry of 20 dB gain Potter Horn Feeding a 150λ Cassegrain

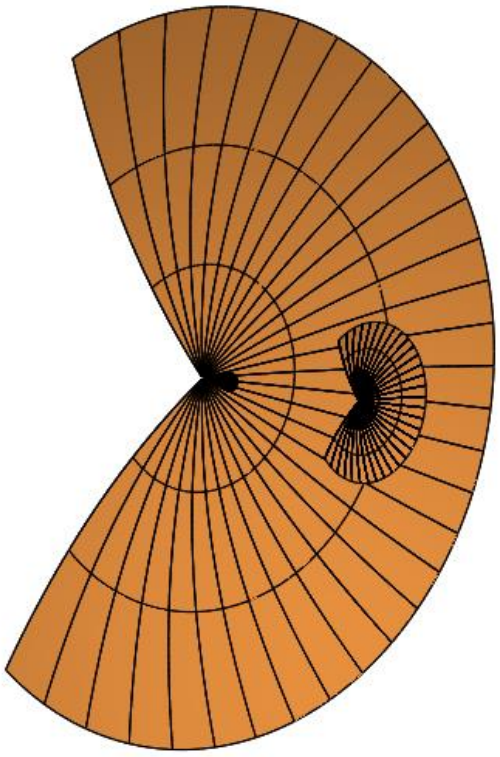

Figure 8-22.21 CHAMP 3d geometry of 20 dB gain Potter Horn Feeding a 150λ Cassegrain

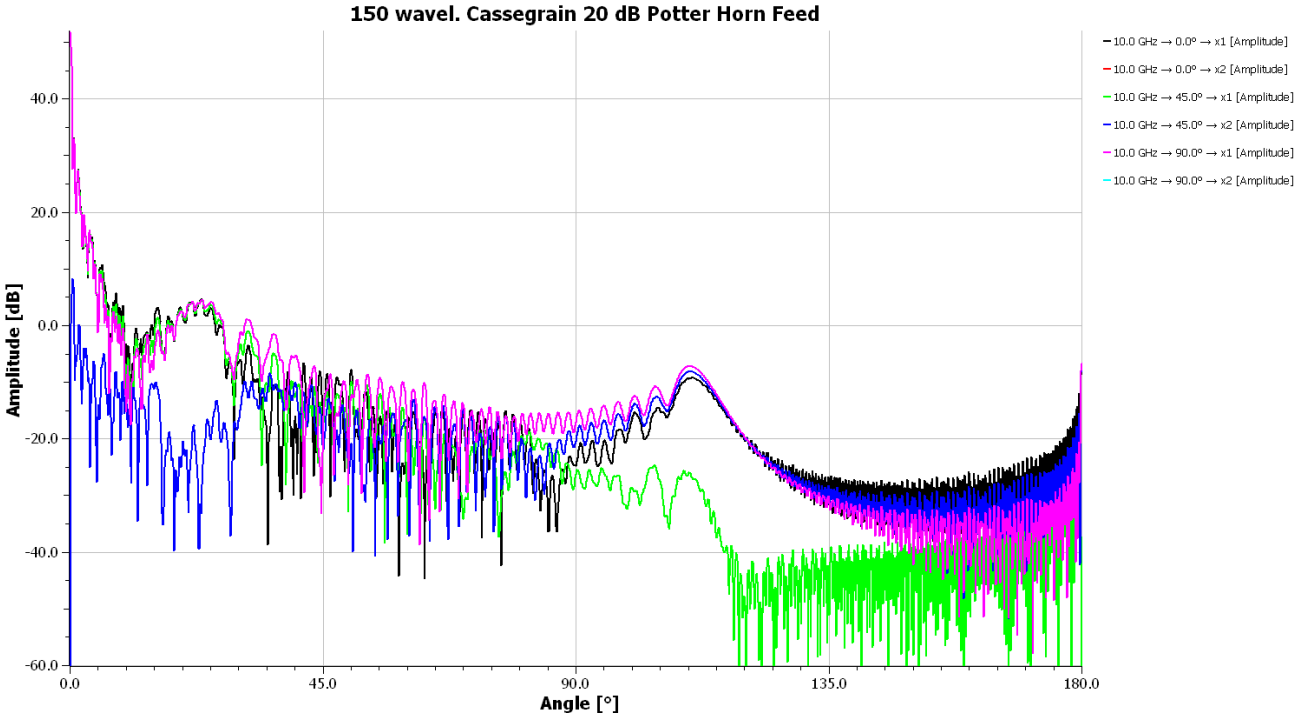

Figure 8-22.23 BOR-MoM analysis of 150λ diameter Cassegrain fed by 20 dB Potter Horn

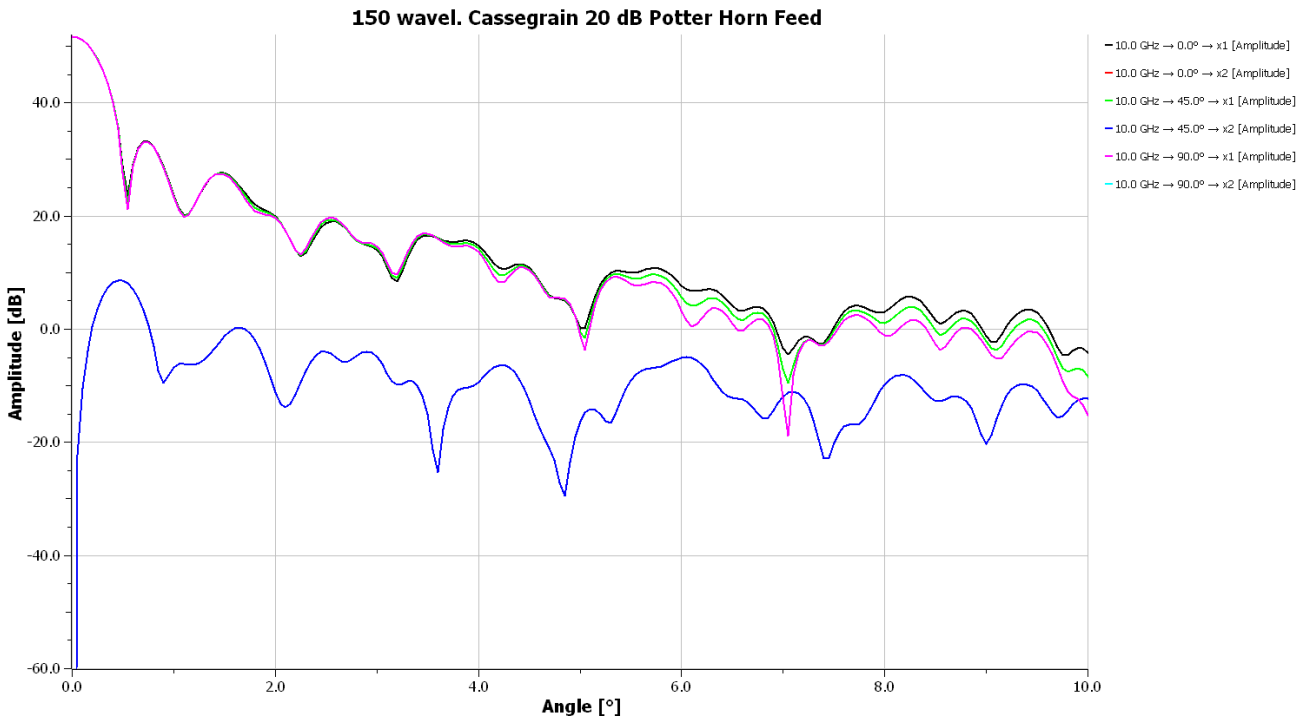

Figure 8-22.24 BOR-MoM analysis of 150λ diameter Cassegrain fed by 20 dB Potter Horn Front lobe

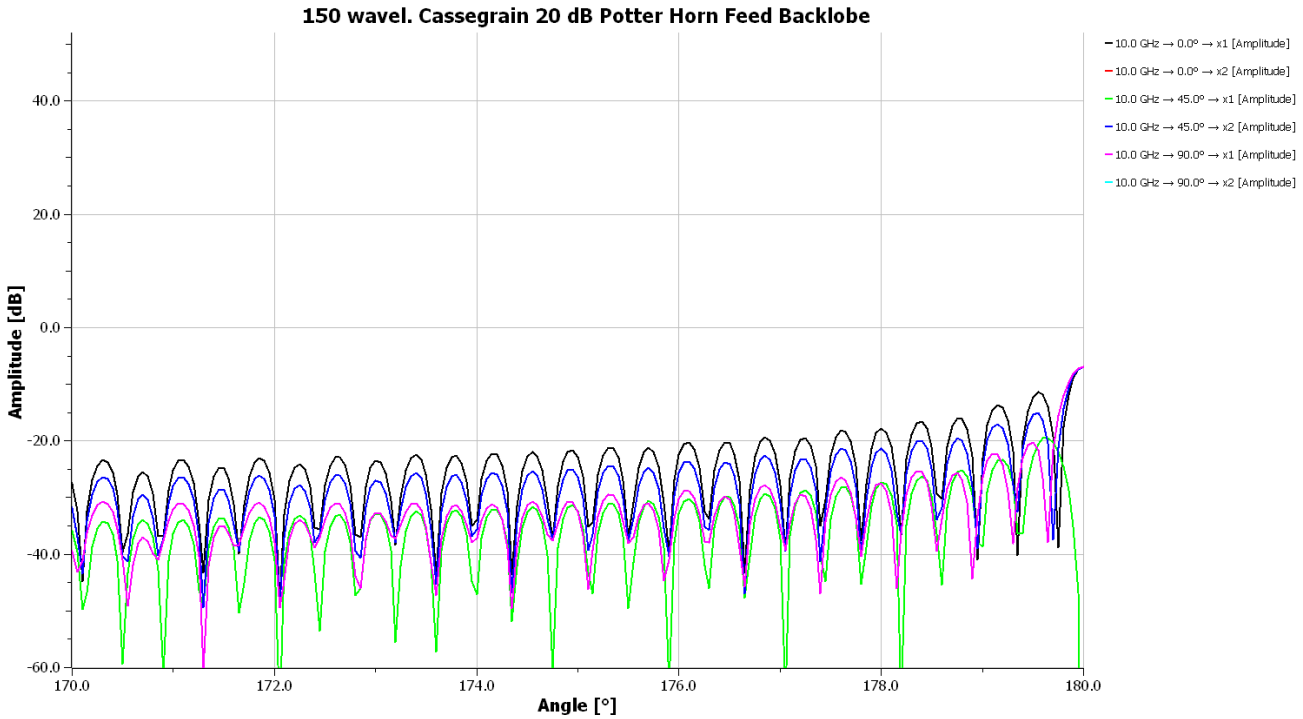

Figure 8-22.25 BOR-MoM analysis of 150λ diameter Cassegrain fed by 20 dB Potter Horn Back lobe

Metal Shroud on Dual Reflector

We use the routine CHESHD to generate a metal shroud by attaching the start point to the edge of the main reflector. The program inputs include the length and angle of the shroud. A metal shroud reduces reflector noise by

shielding spillover radiation on noisy soil and increases G/T. CHESHD geometry.tor addition for the metal shroud does not include reflector offset due to location of the phase center inside the reflector.

```
 ZLOFF  real_variable
(
  value            : 0.0
)

DTR  real_variable
(
  value            : "atan(1.)/45."
)

SHANG  real_variable
(
  value            : 0.0
)

SHLEN  real_variable
(
  value            : 1400.0
)

SHCZ  real_variable
(
  value            : 402.99
)

SHCR  real_variable
(
  value            : 2248.4
)

SHEZ  real_variable
(
  value            : "ref(SHCZ)+cos(ref(SHANG)*ref(DTR))*ref(SHLEN)"
)

SHER  real_variable
(
  value            : "ref(SHCR)+sin(ref(SHANG)*ref(DTR))*ref(SHLEN)"
)

shroud_metal  piecewise_linear_reflector
(
  length_unit      : mm,
  nodes            : table
    (
    "ref(SHCZ)"  "ref(SHCR)"
    "ref(SHEZ)"  "ref(SHER)"
    )
)
```

When we add this to the geometry.tor file using a text editor, we must include the “shroud_metal” in the list of scatterers near the top of the geometry.tor file.

scatterers : sequence(ref(horn_bor_mesh),ref(reflector),ref(reflector_0001),ref(shroud_metal))

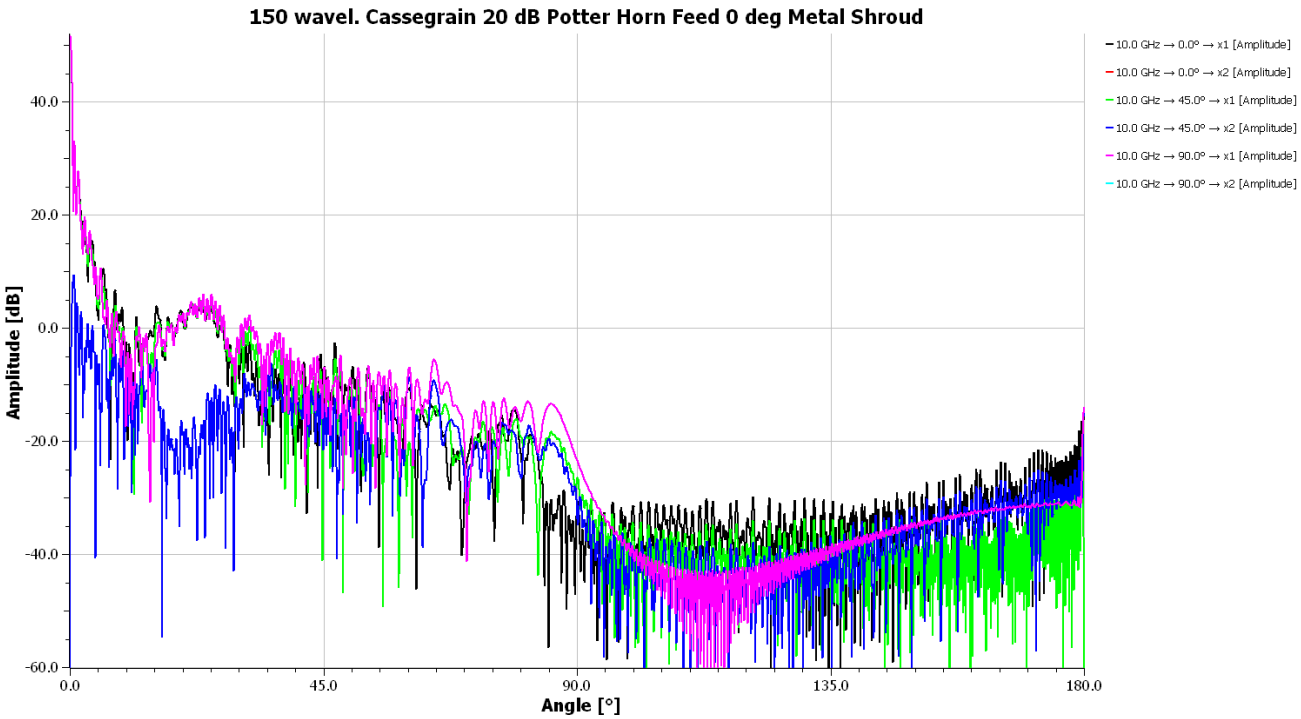

Figure 8-22.26 BOR-MoM analysis of 150λ dia. Cassegrain fed by 20 dB Potter Horn with 0° metal shroud

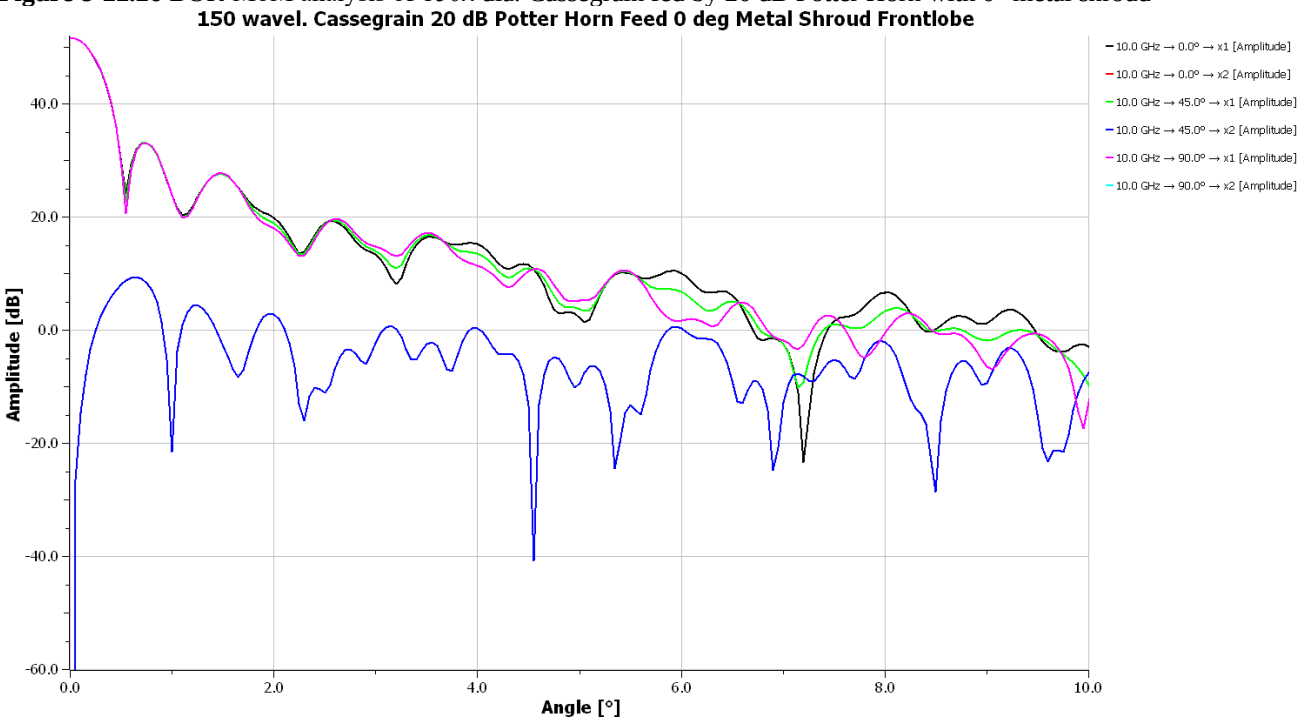

Figure 8-22.27 BOR-MoM analysis of 150λ dia. Cassegrain fed by 20 dB Potter Horn with 0° metal shroud Front lobe

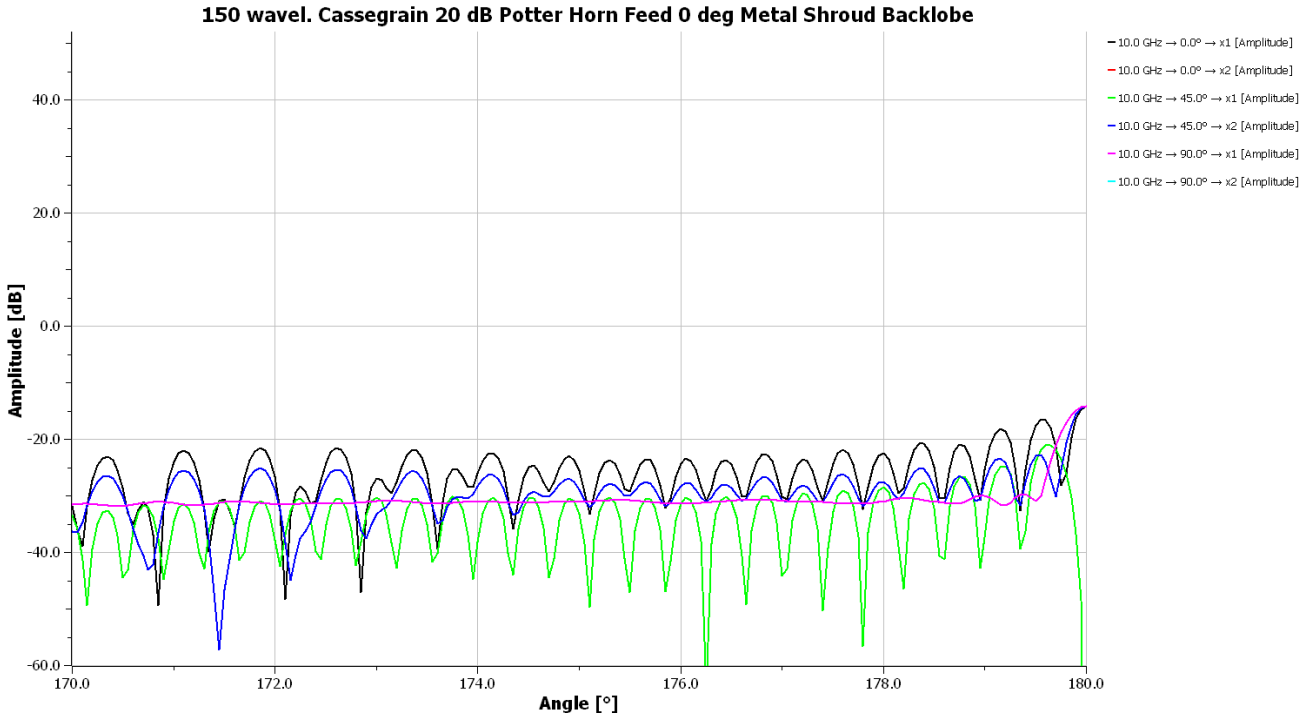

Figure 8-22.28 BOR-MoM analysis of 150λ dia. Cassegrain fed by 20 dB Potter Horn with 0° metal shroud Back lobe

The metal shroud eliminates the spillover lobe and reduces the back lobe. Rotating the shroud by 5° reduced the lobes for the prime focus reflector. We can do the same here by changing the variable SHANG.

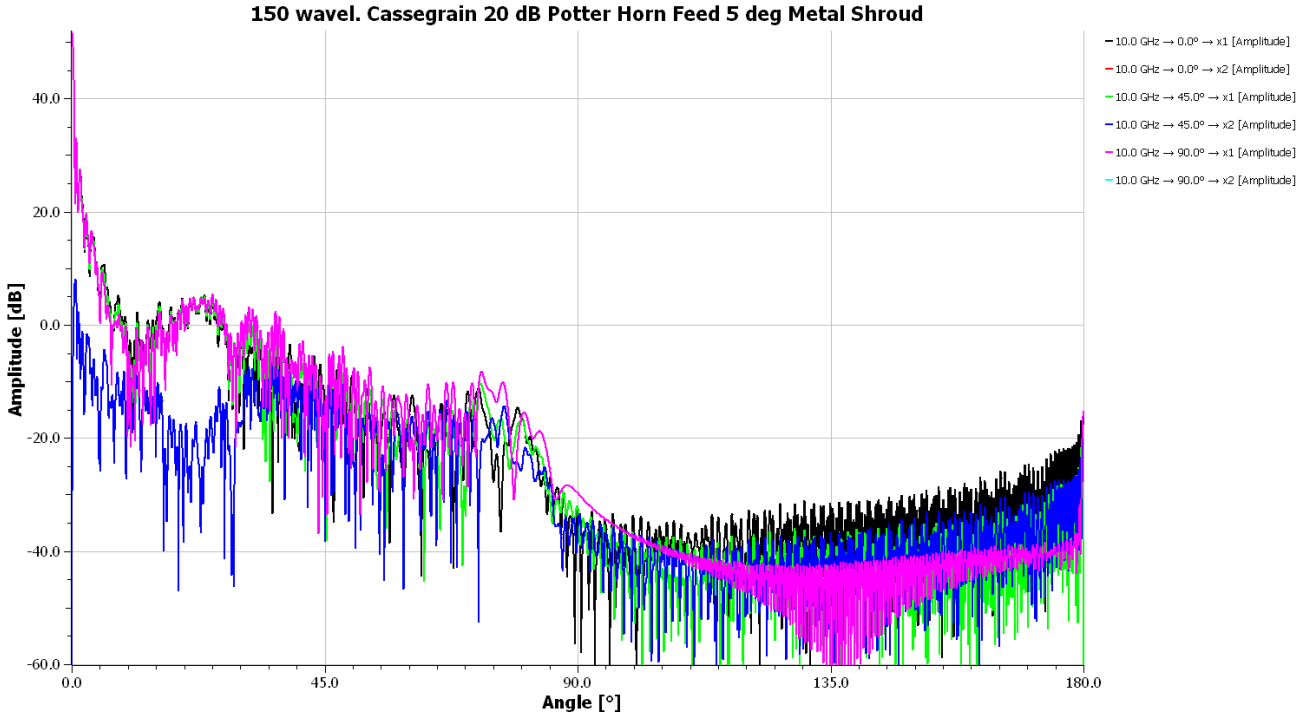

Figure 8-22.29 BOR-MoM analysis of 150λ dia. Cassegrain fed by 20 dB Potter Horn with 5° metal shroud

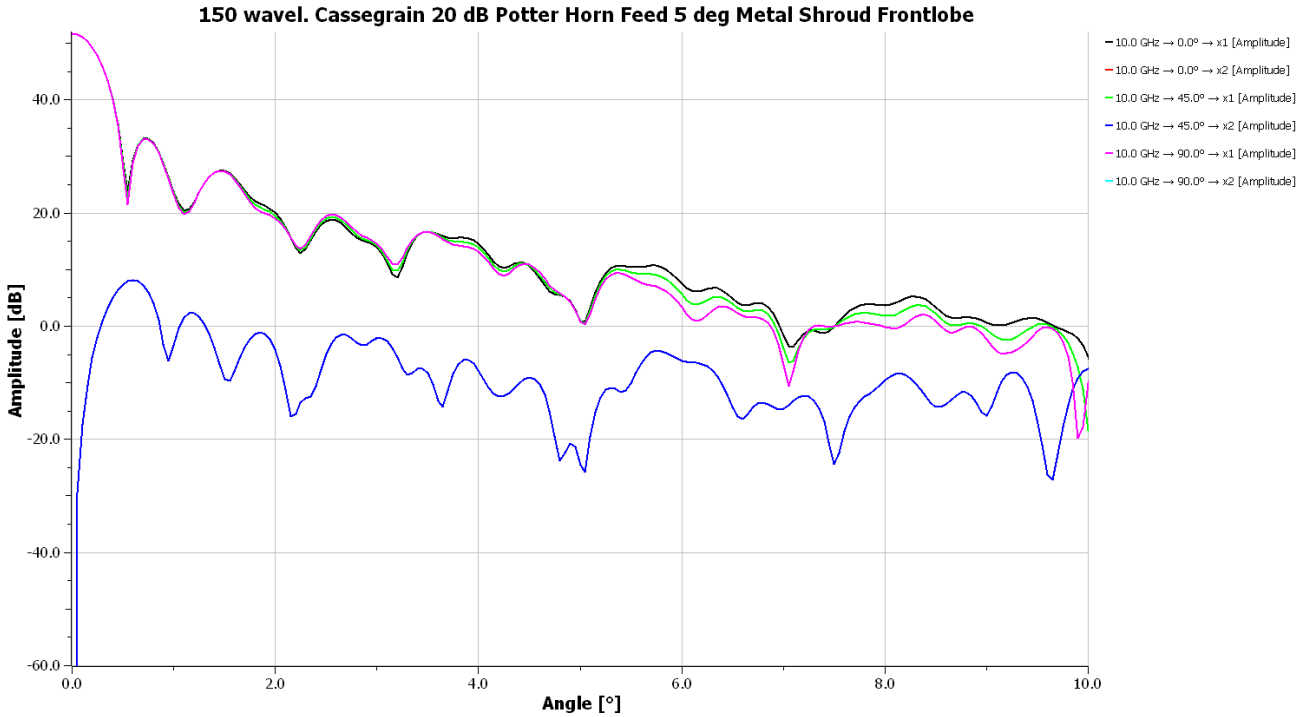

Figure 8-22.30 BOR-MoM analysis of 150λ dia. Cassegrain fed by 20 dB Potter Horn with 0° metal shroud Front lobe

.

The comparison between Figure 8-22.26 and 8-22.29 shows small improvements in the spillover region and in the back lobe. The front lobe has changed little. The last 10° of the back lobe produces only small changes between the two orientations (0° and 5°).

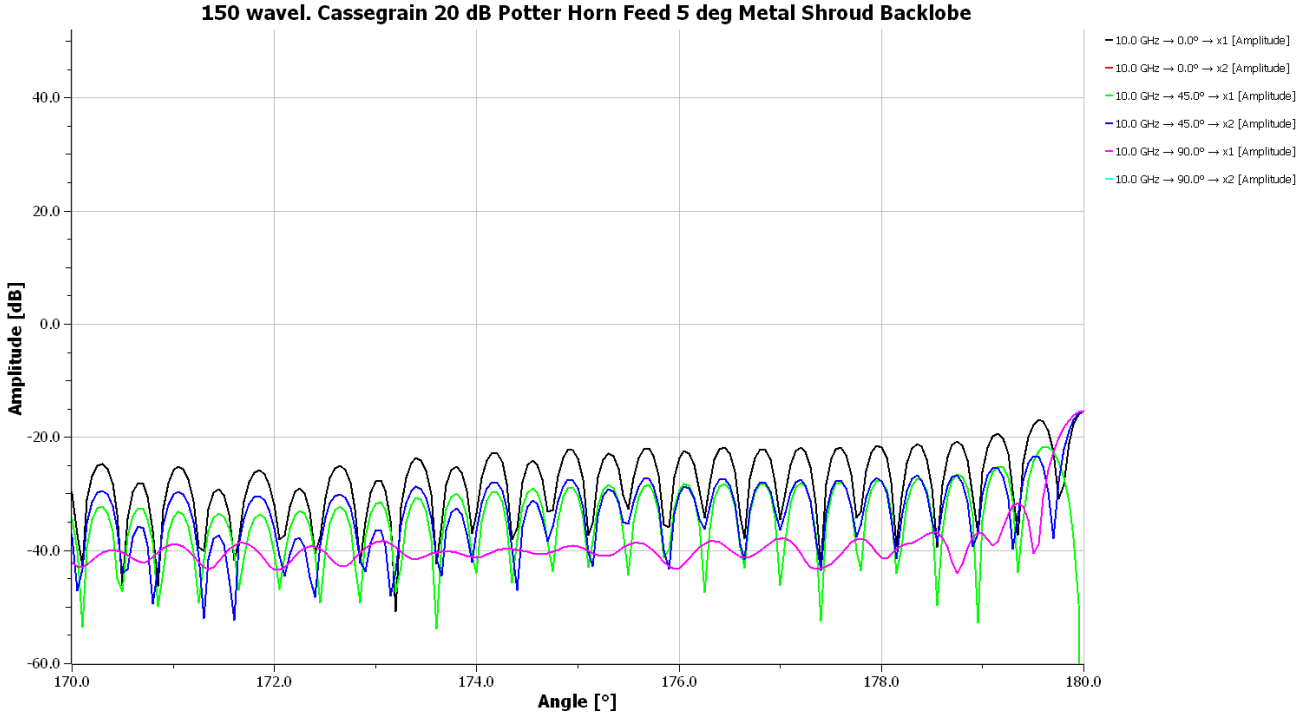

Figure 8-22.31 BOR-MoM analysis of 150λ dia. Cassegrain fed by 20 dB Potter Horn with 0° metal shroud Back lobe

The program CHASHD generates the addition to the geometry.tor file for an absorber lined shroud of a dual reflector with the angle of the shroud as 0°. The absorber reduces the spillover region to about -40 dBi.

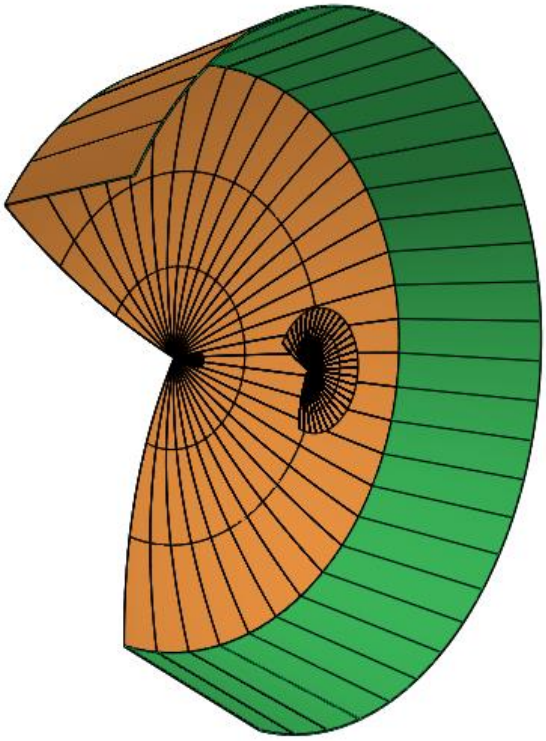

Figure 8-22.32 150λ dia. Cassegrain with Absorber Lined Shroud

The thin absorber layer great increases runtime with multiple thin layers increasing runtime even more.

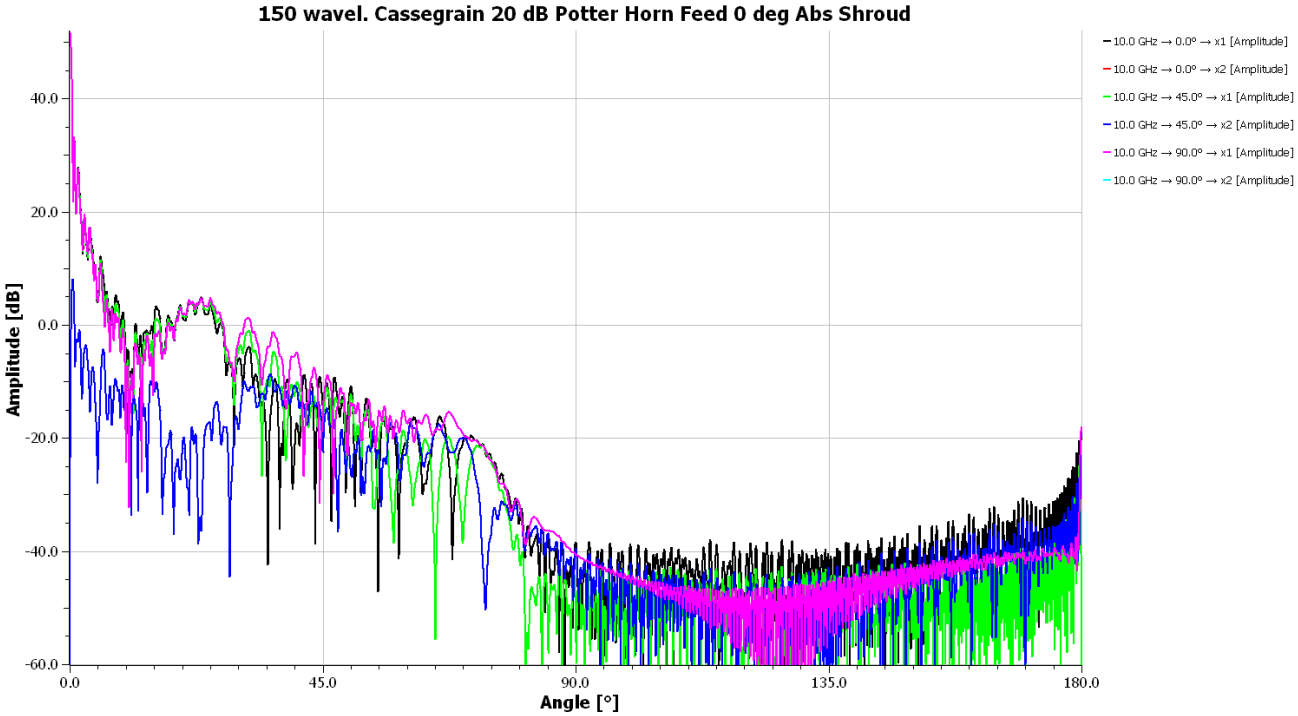

Figure 8-22.33 BOR-MoM analysis of 150λ dia. Cassegrain fed by 20 dB Potter Horn with 0° absorber lined shroud

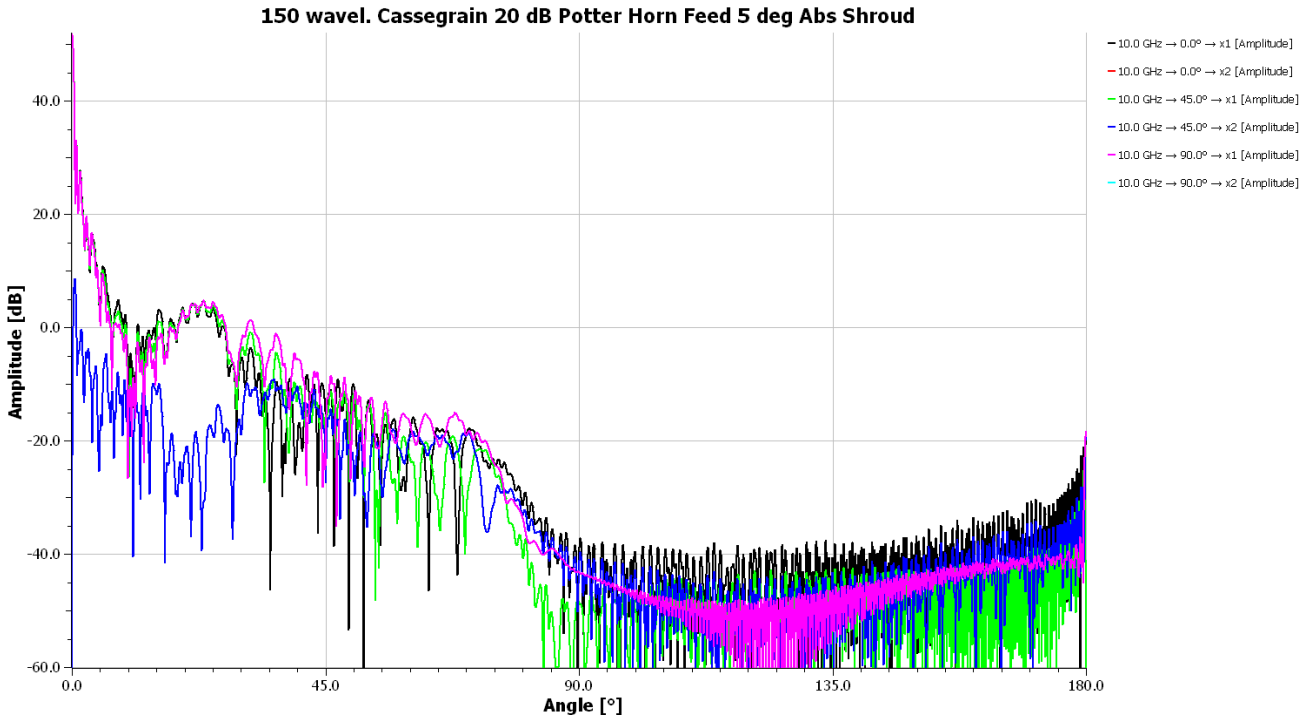

Figure 8-22.34 BOR-MoM analysis of 150λ dia. Cassegrain fed by 20 dB Potter Horn with 5° absorber lined shroud

Figures 8-22.33 and 8-22.34 are very similar and show that the angle of the shroud has little effect.

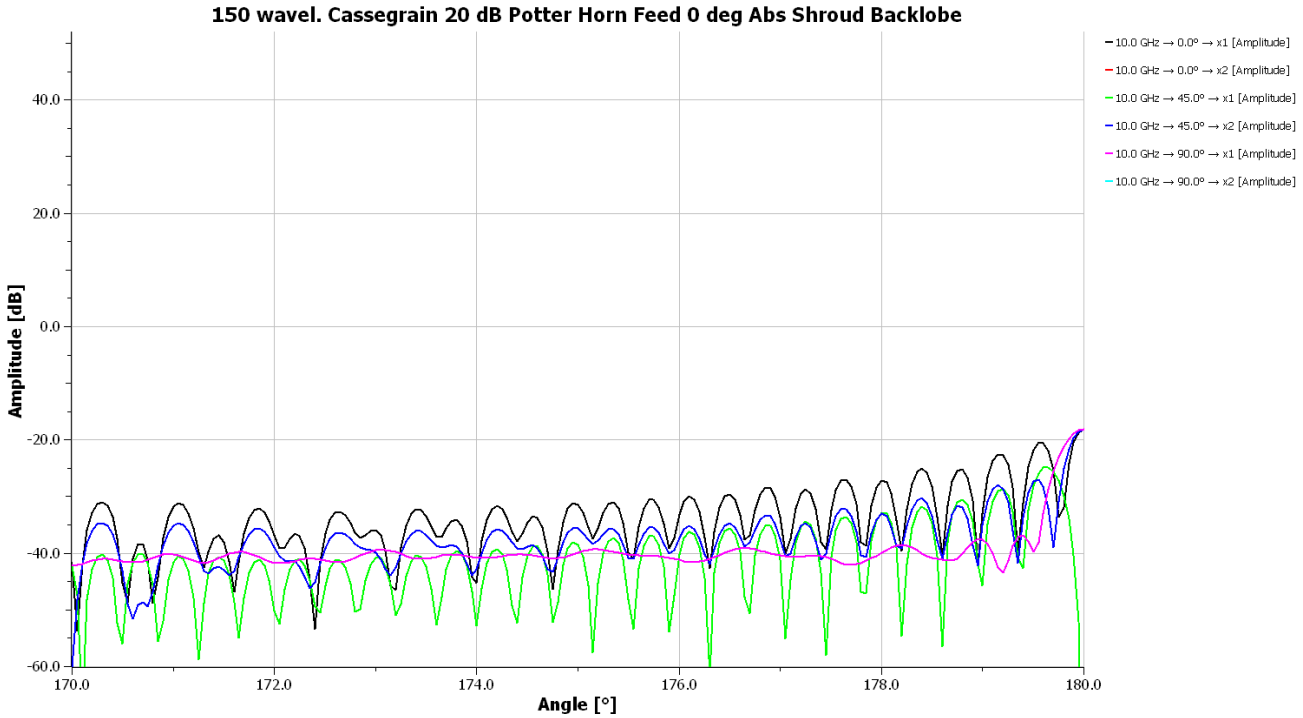

Figure 8-22.35 BOR-MoM analysis of 150λ dia. Cassegrain fed by 20 dB Potter Horn with 0° absorber lined shroud Back lobe

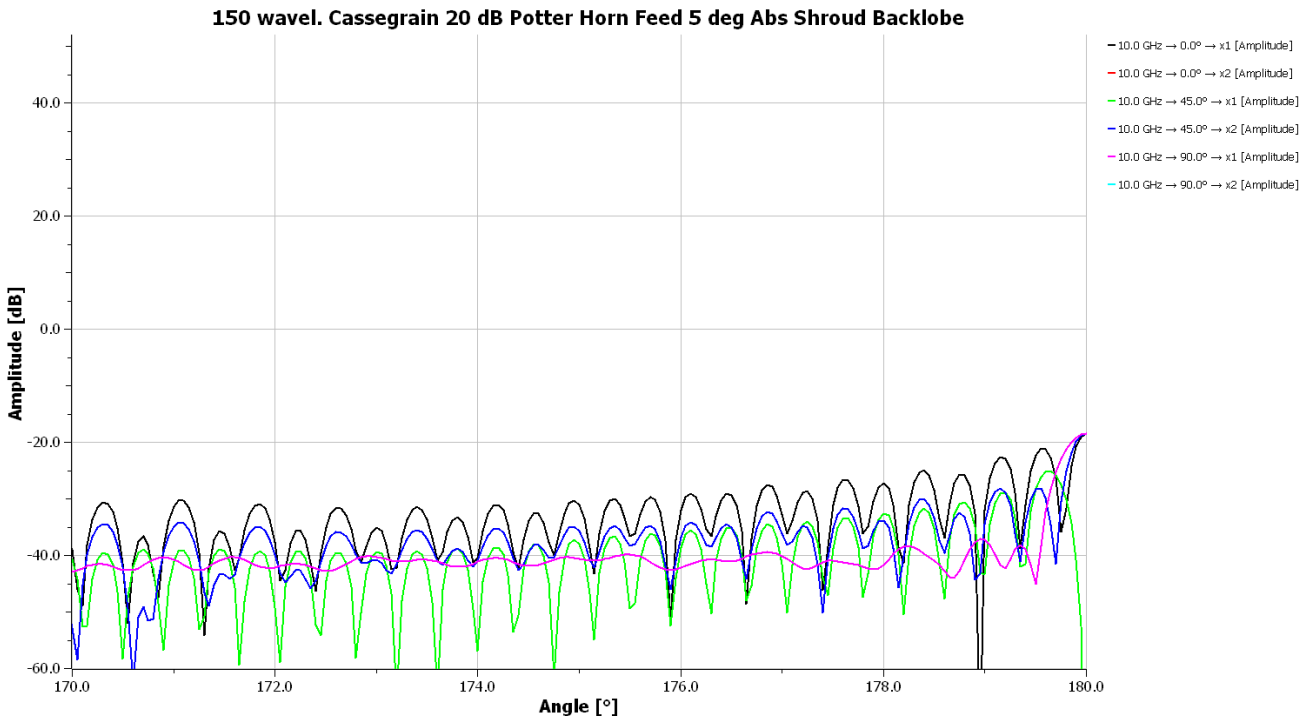

Figure 8-22.36 BOR-MoM analysis of 150λ dia. Cassegrain fed by 20 dB Potter Horn with 5° absorber lined shroud Back lobe

Radomes for Reflectors using BOR-MoM Analysis

Only reflectors with axisymmetric radomes can be analyzed with BOR-MoM. Some axisymmetric reflectors with shrouds extend it so it is antisymmetric with a sloping cover. The techniques of this section will give first order approximations to these designs.

Radomes consisting of combinations straight line cones and curved cones have been developed.

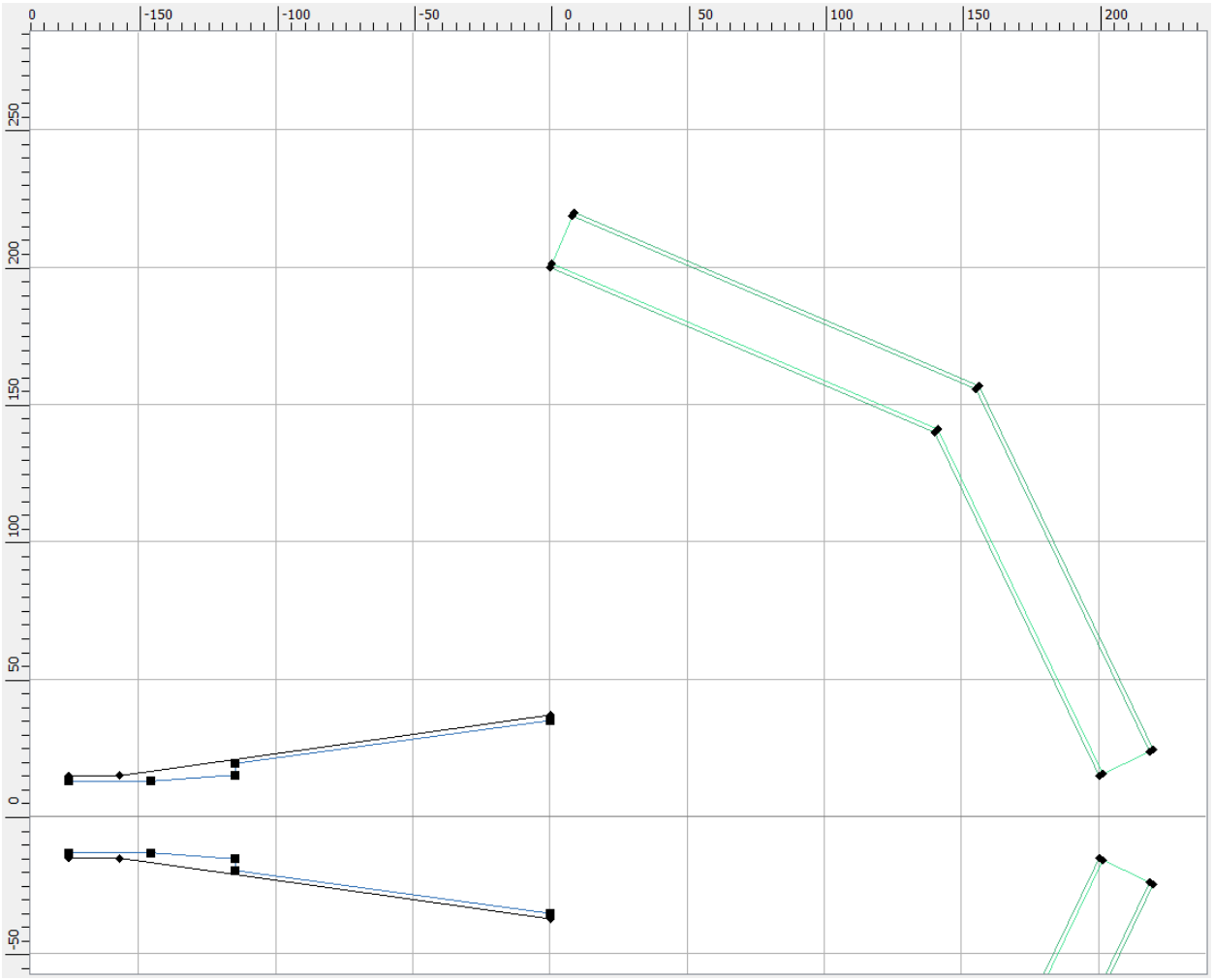

Figure 8-22.37 16-dB Gain Potter Horn with straight line sections A-sandwich Radome

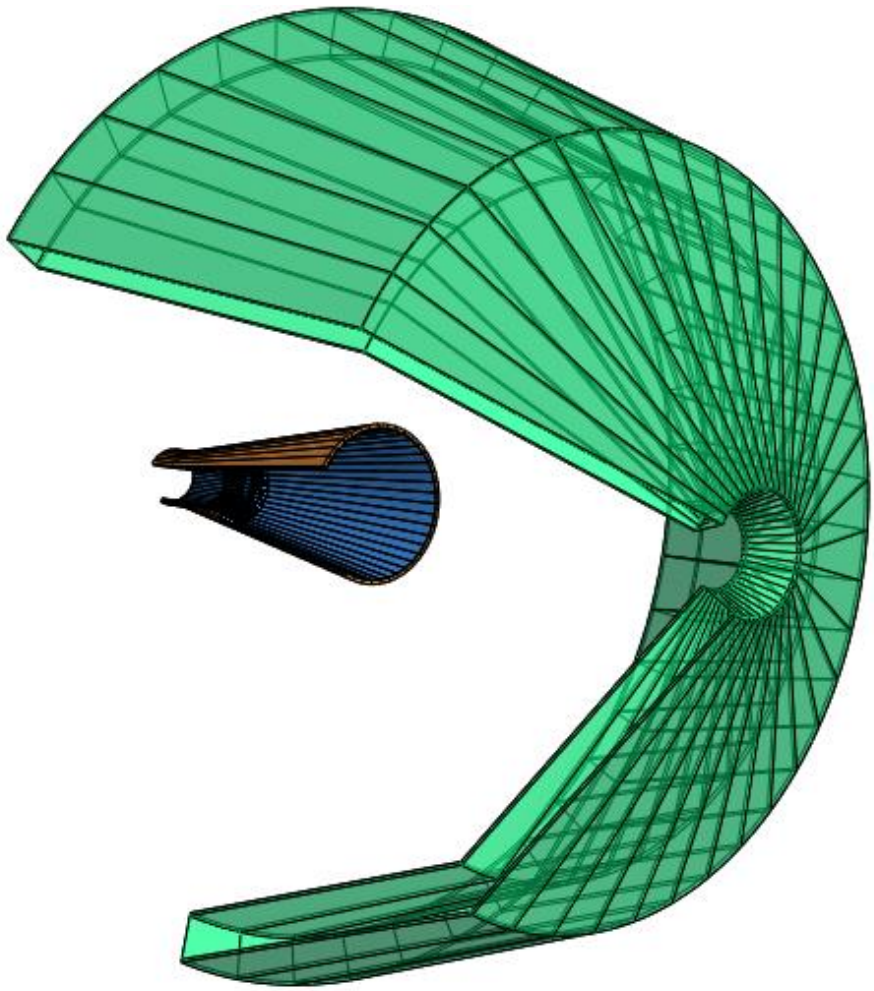

Figure 8-22.38 16-dB Gain Potter Horn with straight line sections A-sandwich Radome

This example leaves a small hole at boresight to prevent overlap across the *z*-axis, although it could be smaller than shown. The program CHIRAD generates a bor_mesh addition to the geometry.tor CHAMP file for multilayer radomes consisting of straight line sections. Either the inner or outer layer is defined by a series of points. The multiple radome layers either move outer or inner. The layer intersections generate long text lines in the geometry.tor files for nodes because CHAMP variables are used to specify the radome. Below is the bor_mesh for the radome shown above.

```
radome_16            bor_mesh
(
  regions           : table
   (
        1  4.0000E+00  1.0000E+00  2.0000E-02
        2  2.0000E+00  1.0000E+00  4.0000E-02
   ),
  nodes             : table
   (
        1  0.00000E+00  2.00000E+02
        2  1.40000E+02  1.40000E+02
        3  2.00000E+02  1.50000E+01
        4   "  0.0000E+00-ref(UVR1)*ref(TT1)"   "  2.0000E+02+ref(UVZ1)*ref(TT1)"
```

```
        5   "  0.0000E+00-ref(UVR1)*ref(TT1)+ref(UVZ1)*(ref(UVR2)*(  0.0000E+00-
2.0000E+02+(ref(UVR2)-ref(UVR1))*ref(TT1))+ref(UVZ2)*(  1.5000E+01-
2.0000E+02+(ref(UVZ2)-ref(UVZ1))*ref(TT1)))/ref(DET1)"   "
2.0000E+02+ref(UVZ1)*ref(TT1)+ref(UVR1)*(ref(UVR2)*(  0.0000E+00-
2.0000E+02+(ref(UVR2)-ref(UVR1))*ref(TT1))+ref(UVZ2)*(  1.5000E+01-
2.0000E+02+(ref(UVZ2)-ref(UVZ1))*ref(TT1)))/ref(DET1)"
        6   "  2.0000E+02-ref(UVR2)*ref(TT1)"   "  1.5000E+01+ref(UVZ2)*ref(TT1)"
        7   "  0.0000E+00-ref(UVR1)*ref(TT2)"   "  2.0000E+02+ref(UVZ1)*ref(TT2)"
        8   "  0.0000E+00-ref(UVR1)*ref(TT2)+ref(UVZ1)*(ref(UVR2)*(  0.0000E+00-
2.0000E+02+(ref(UVR2)-ref(UVR1))*ref(TT2))+ref(UVZ2)*(  1.5000E+01-
2.0000E+02+(ref(UVZ2)-ref(UVZ1))*ref(TT2)))/ref(DET1)"   "
2.0000E+02+ref(UVZ1)*ref(TT2)+ref(UVR1)*(ref(UVR2)*(  0.0000E+00-
2.0000E+02+(ref(UVR2)-ref(UVR1))*ref(TT2))+ref(UVZ2)*(  1.5000E+01-
2.0000E+02+(ref(UVZ2)-ref(UVZ1))*ref(TT2)))/ref(DET1)"
        9   "  2.0000E+02-ref(UVR2)*ref(TT2)"   "  1.5000E+01+ref(UVZ2)*ref(TT2)"
    ),
  linear_segments        : table
    (

          1     1     2   0   1   -1.0    0.0
          2     2     3   0   1   -1.0    0.0
          3     4     5   1   2   -1.0    0.0
          4     5     6   1   2   -1.0    0.0
          5     7     8   2   0   -1.0    0.0
          6     8     9   2   0   -1.0    0.0
          7     1     4   0   1   -1.0    0.0
          8     3     6   0   1   -1.0    0.0
          9     4     7   0   2   -1.0    0.0
         10     6     9   0   2   -1.0    0.0
    ),
  length_unit       : mm
  )
```

The three layer radome was design to minimize transmission loss at 0° incidence and high angle of incidence causes significant distortion, as shown below. The thickness of the radome layers are variables in CHAMP so the transmission through the radome can be optimized.

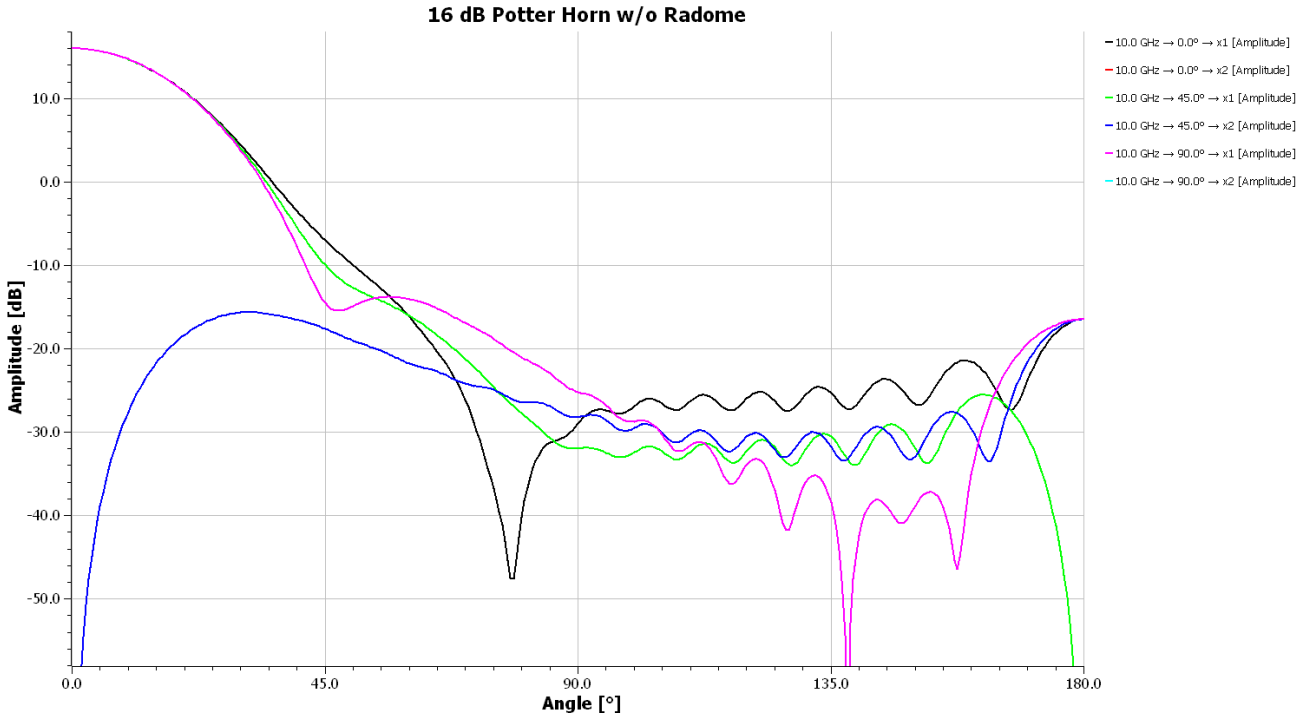

Figure 8-22.39 16 dB Gain Potter Horn without Radome

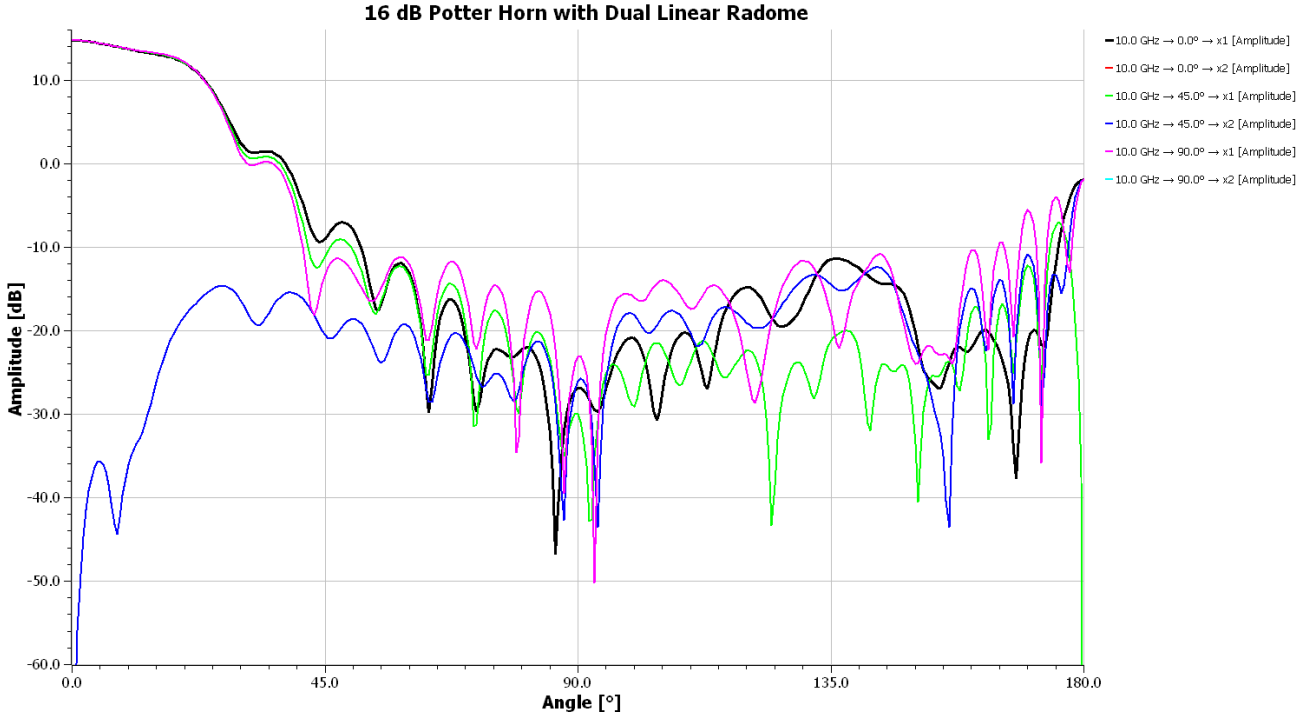

Figure 8-22.40 16 dB Gain Potter Horn with Radome with Linear Sections (Figure 8-22.38)

A second type of radome uses curved splines in the bor_mesh. The program CHCURAD accepts a few points (~8 to 10) in a list and generates cubic splines for groups of 4 points each along the inner or outer layer. The spline between points uses length along the curve as its independent variable, which approximates the arc length parameterization of differential geometry. The derivative with respect to this parameter produces the approximate unit tangent vector. Rotation of this vector by 90° gives the unit normal used to determine the points of other layer boundaries.

A circle centered on the aperture generates the following radome in front of the 16-dB gain Potter horn.

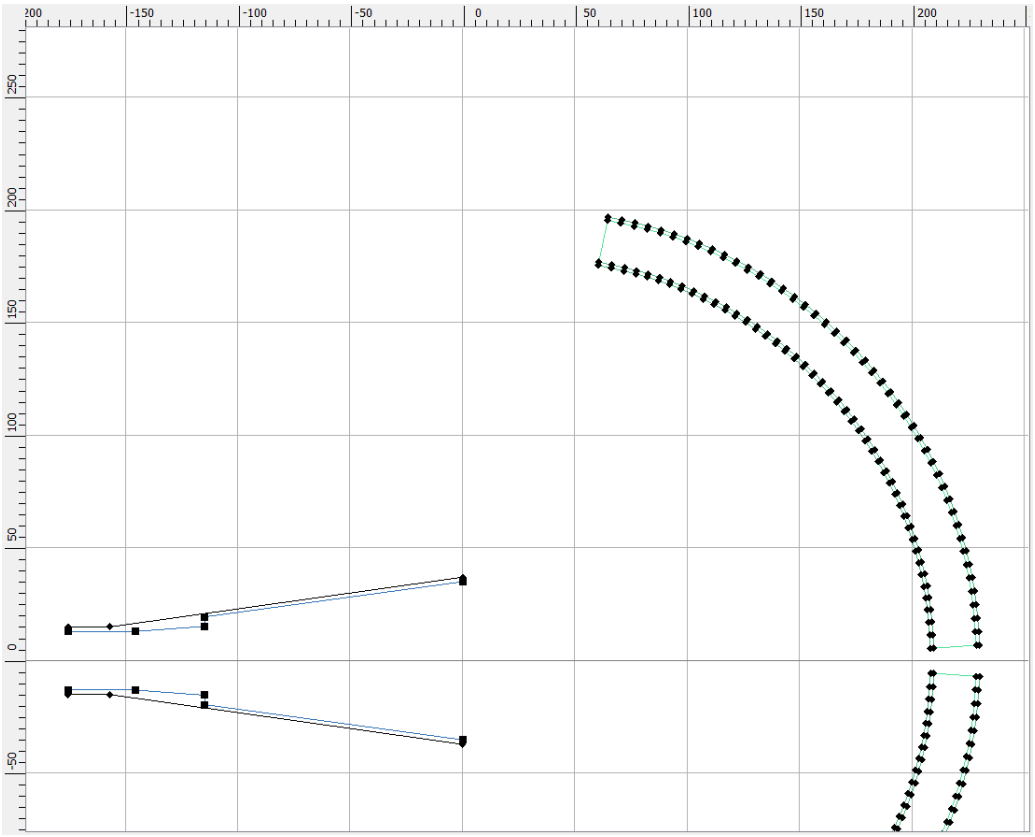

Figure 8-22.41 16-dB Gain Potter Horn with circular (spherical) A-sandwich Radome

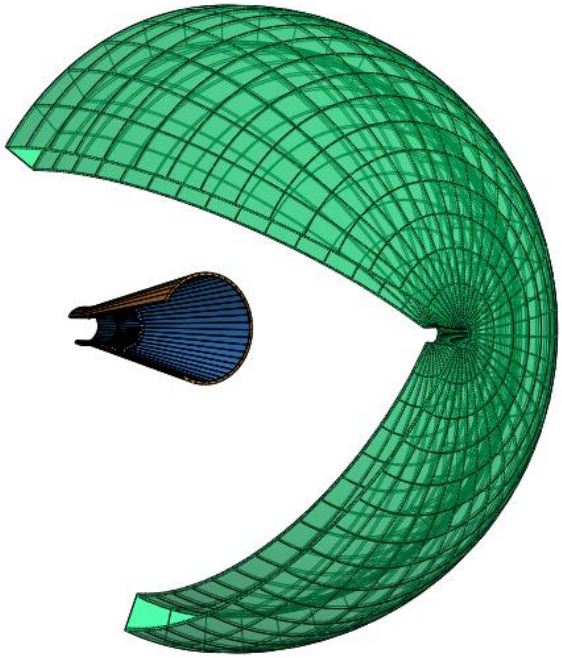

Figure 8-22.42 16-dB Gain Potter Horn with circular (spherical) A-sandwich Radome

The spherical radome has little effect on the pattern.

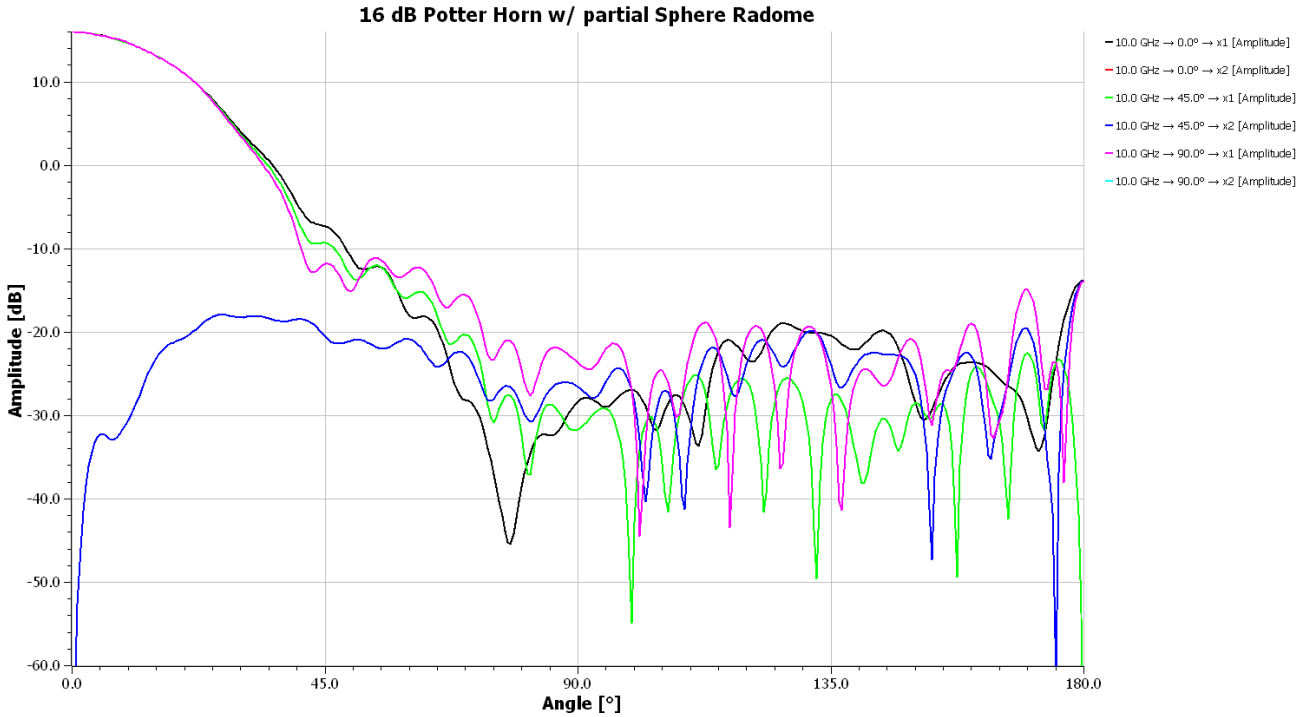

Figure 8-22.43 16 dB Gain Potter Horn with Spherical A-sandwich Radome (Figure 8-22.42)

The program CRADPTS generates the list of points for spherical, conic sections, and sinusoidal surfaces for input to CHCURAD.

Radomes with Cassegrain Dual Reflector

The radome can be used to support the subreflector. We give two simple cases where the radome joins the edge of a metal shroud to the subreflector.

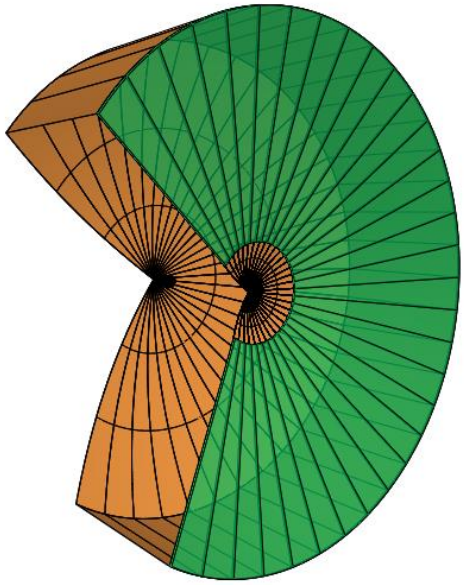

Figure 8-22.44 Linear Radome supports Subreflector in 150λ dia. Cassegrain w/ Metal Shroud

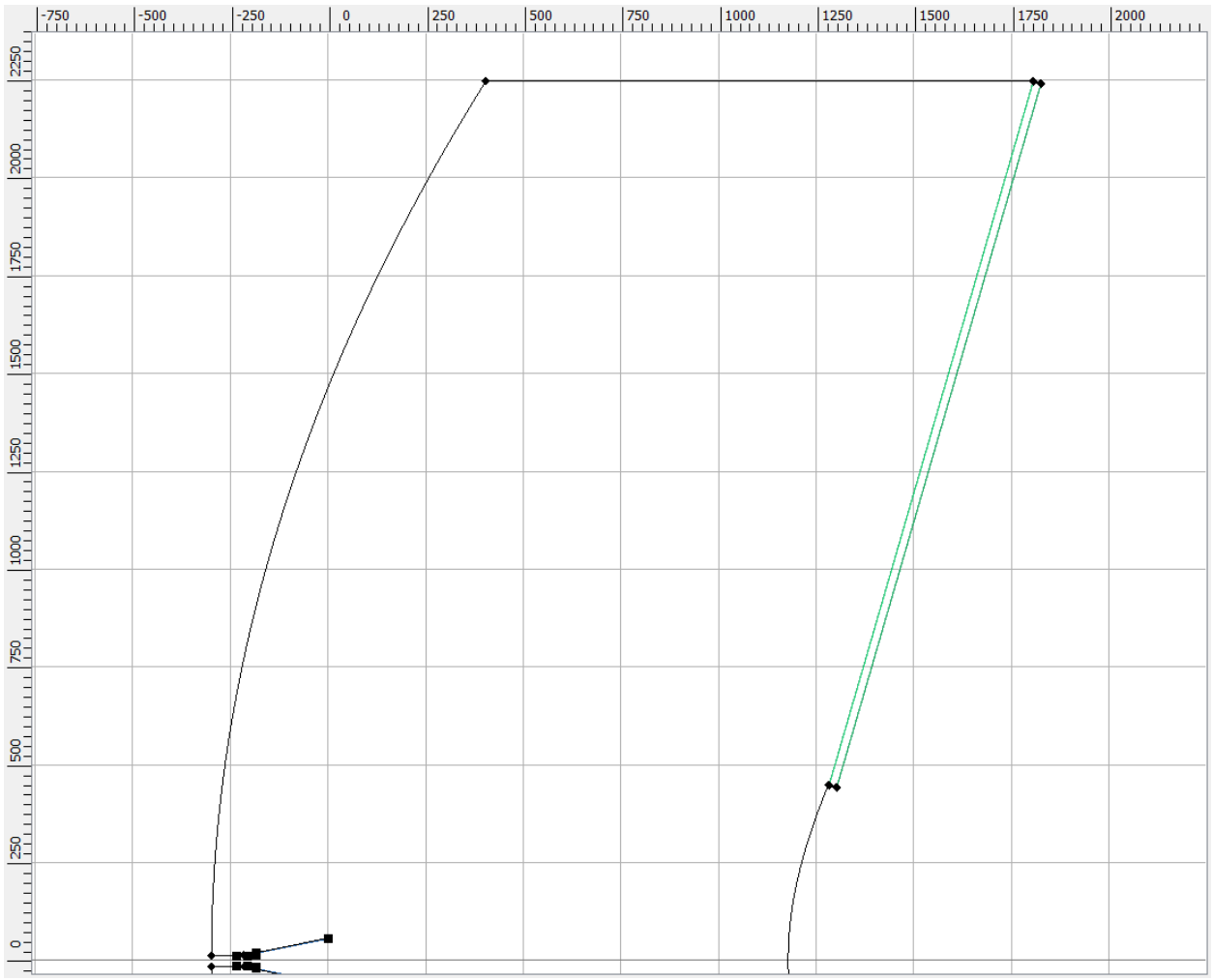

Figure 8-22.45 Linear Radome supports Subreflector in 150λ dia. Cassegrain w/ Metal Shroud

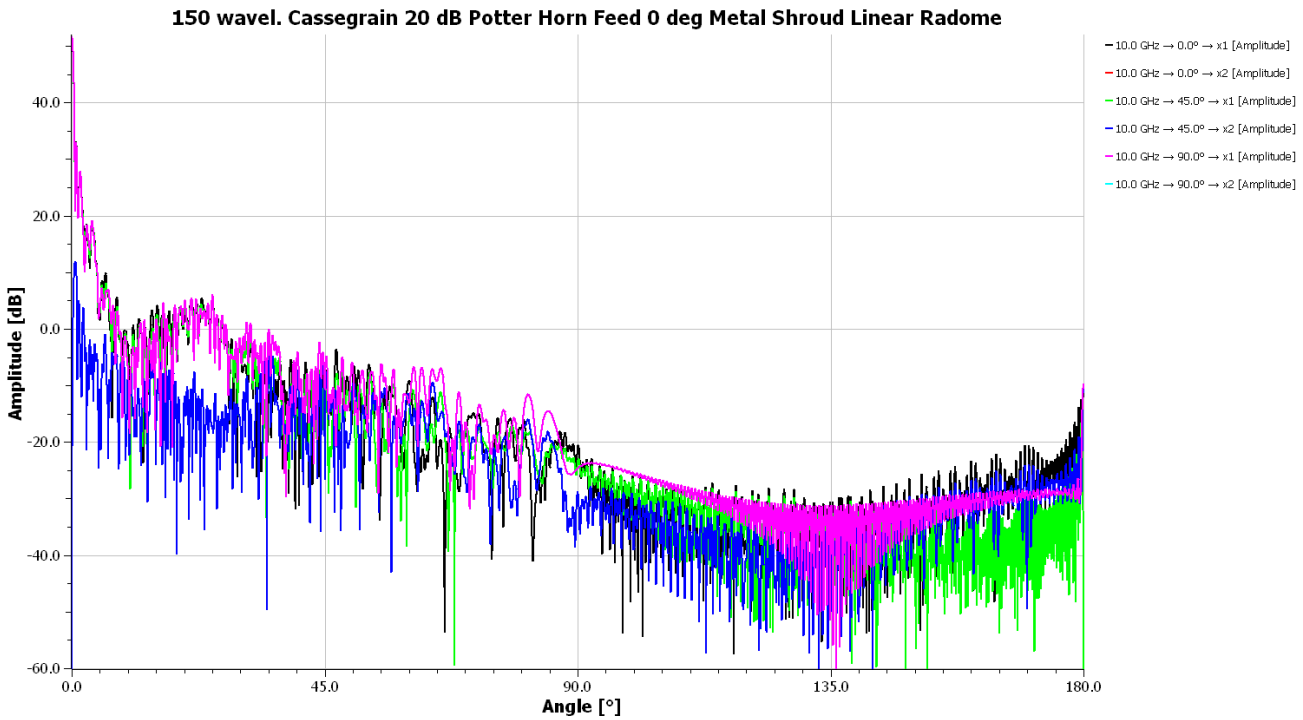

Figure 8-22.46 BOR-MoM analysis of 150λ dia. Cassegrain fed by 20 dB Potter Horn with 0° metal shroud and Linear Cone radome support

The radome increases the back lobe level.

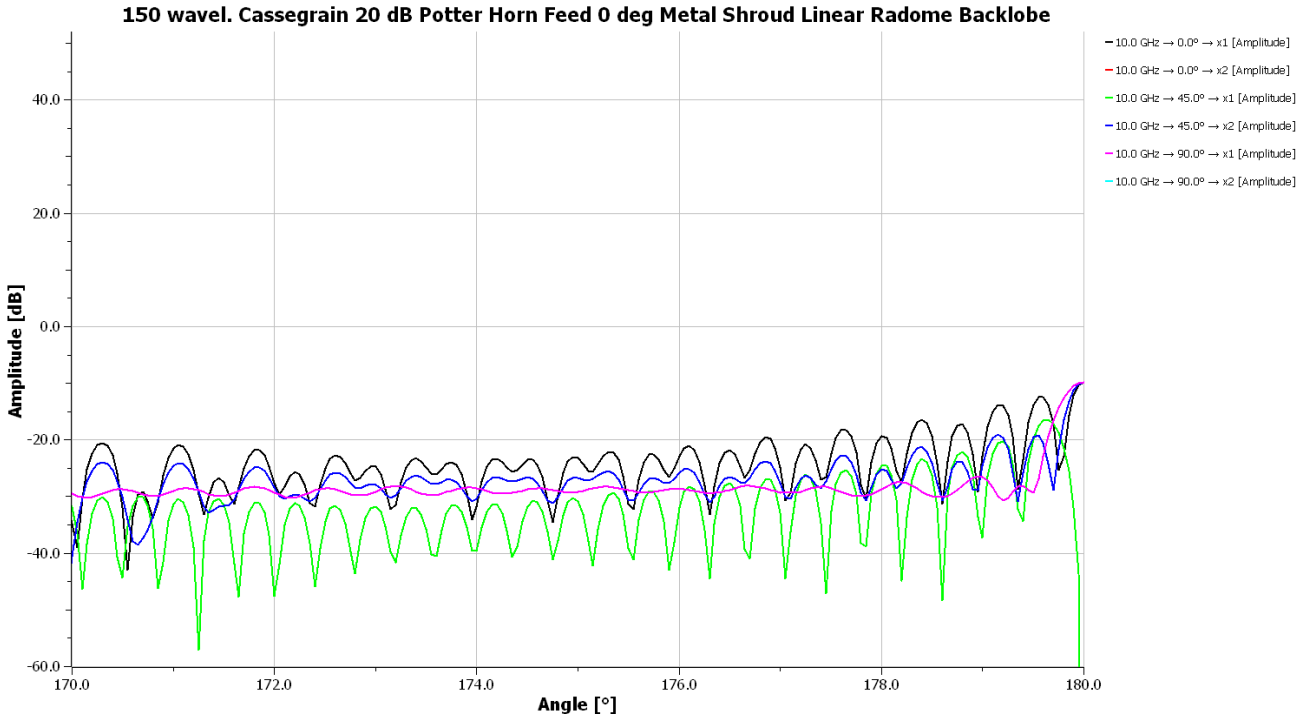

Figure 8-22.47 BOR-MoM analysis of 150λ dia. Cassegrain fed by 20 dB Potter Horn with 0° metal shroud and Linear Cone radome support Back Lobe

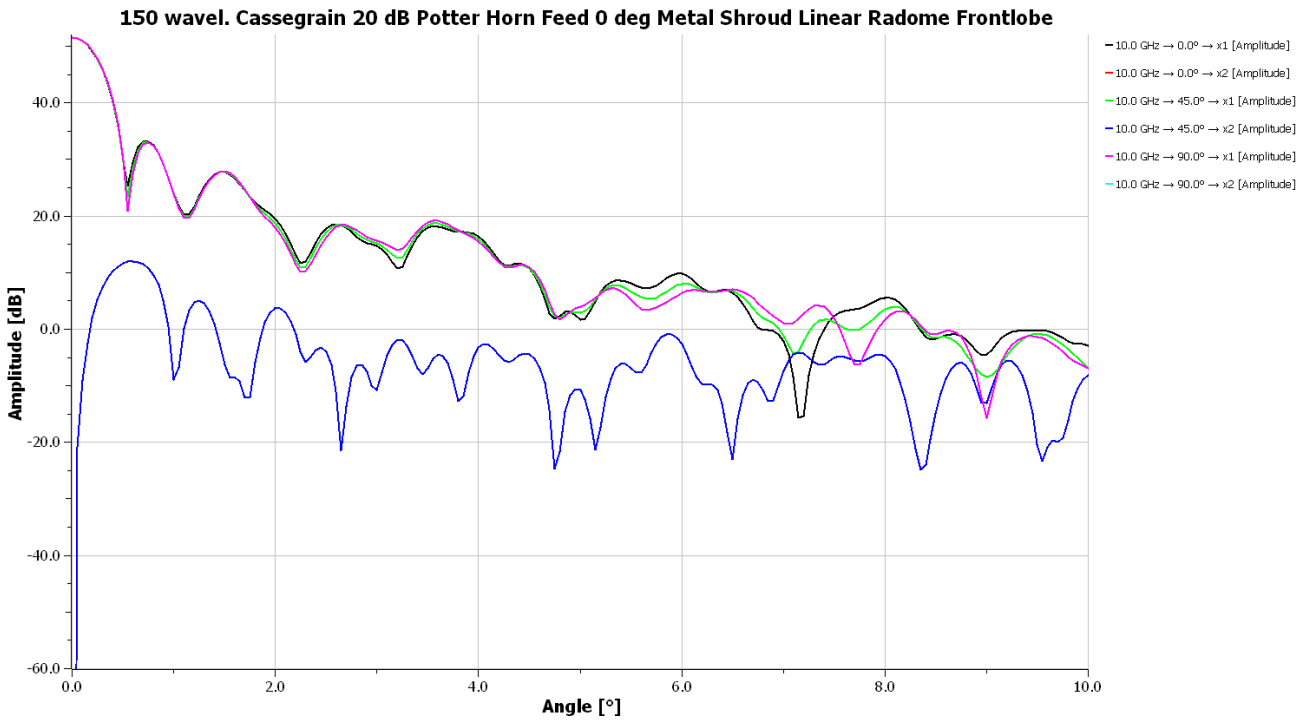

Figure 8-22.48 BOR-MoM analysis of 150λ dia. Cassegrain fed by 20 dB Potter Horn with 0° metal shroud and Linear Cone radome support Front Lobe

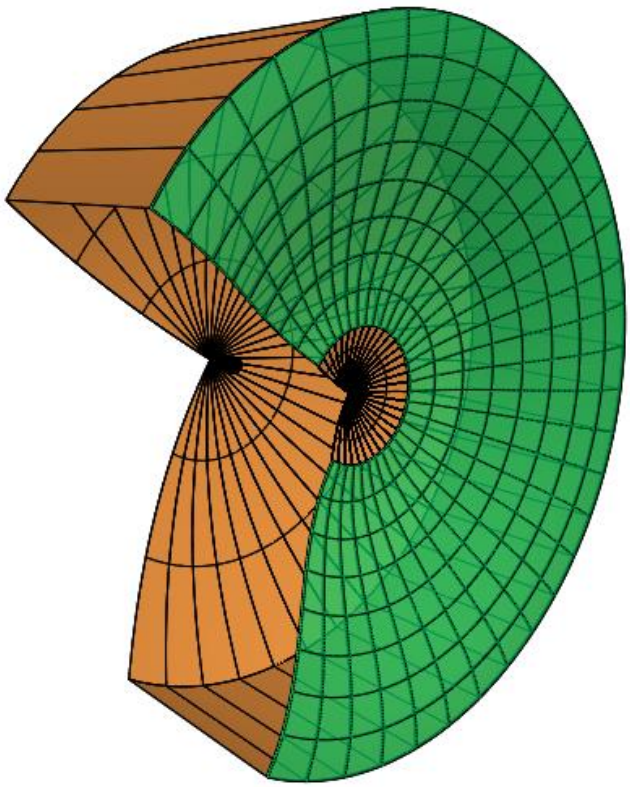

Figure 8-22.49 Sinusoidal Radome supports Subreflector in 150λ dia. Cassegrain w/ Metal Shroud

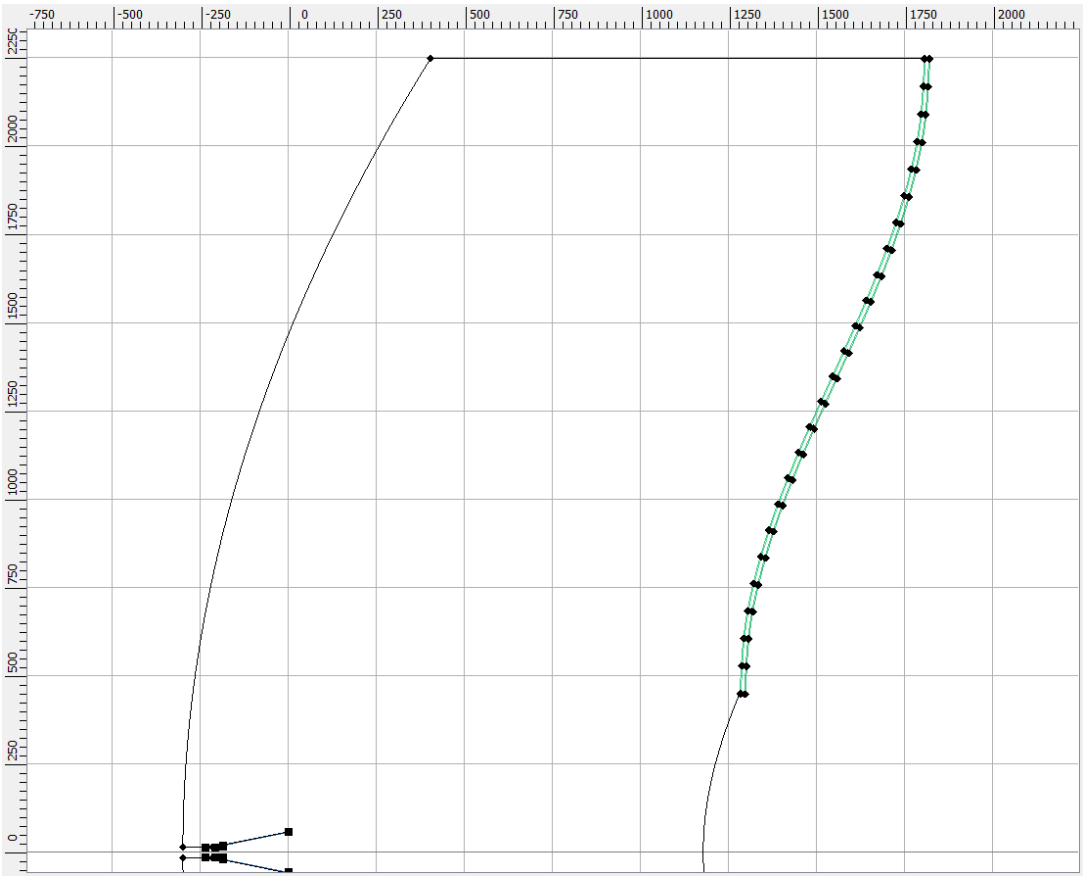

Figure 8-22.50 Sinusoidal Radome supports Subreflector in 150λ dia. Cassegrain w/ Metal Shroud

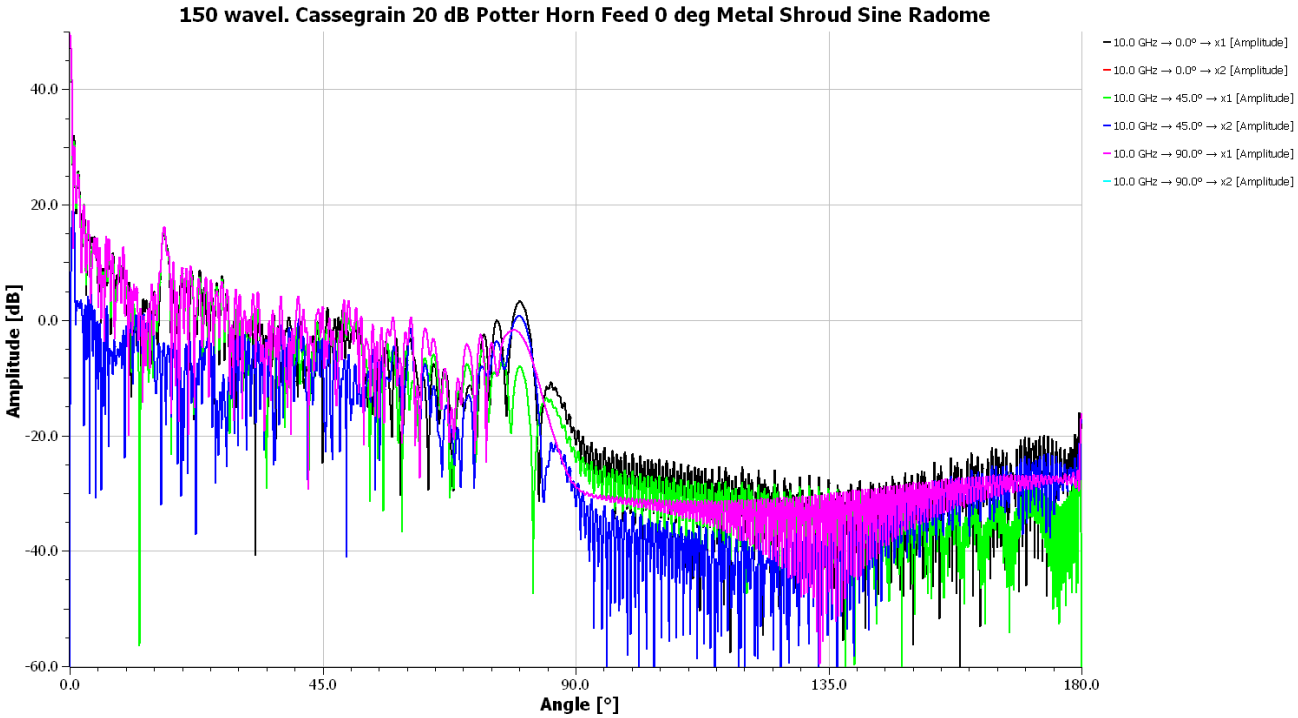

Figure 8-22.51 BOR-MoM analysis of 150λ dia. Cassegrain fed by 20 dB Potter Horn with 0° metal shroud and Sinusoidal Cone radome support

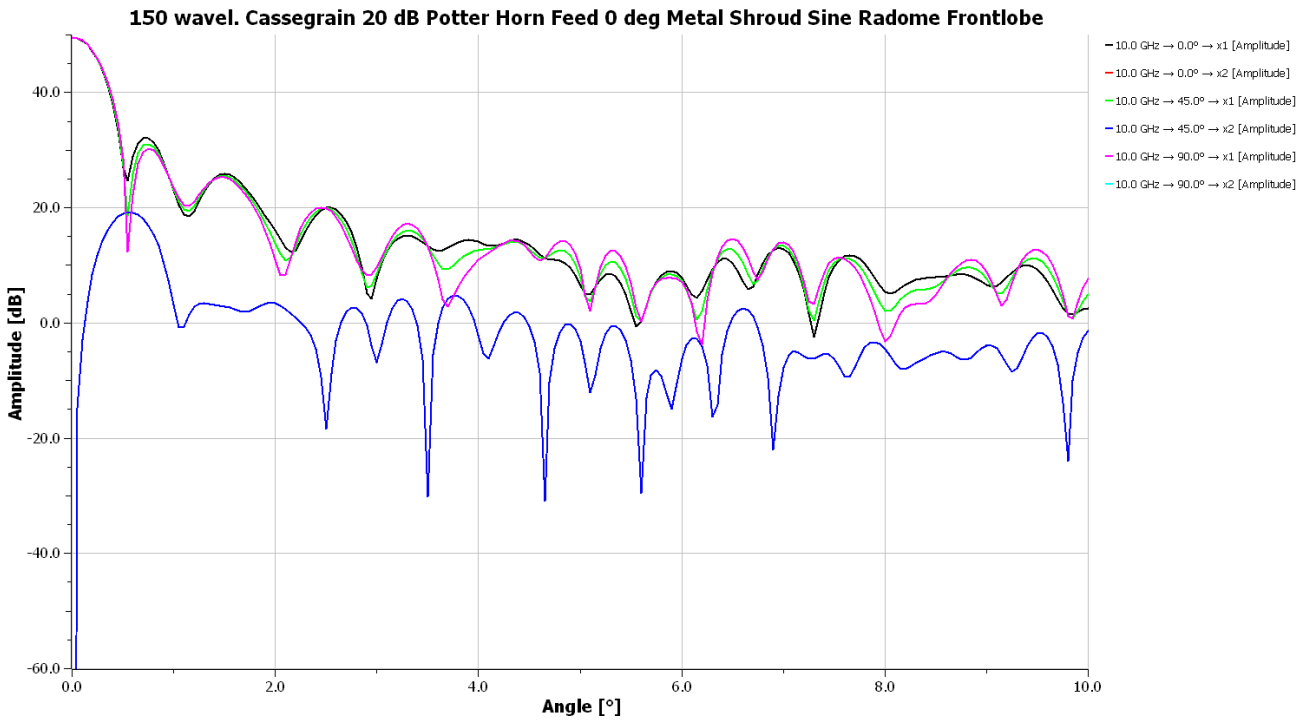

Figure 8-22.52 BOR-MoM analysis of 150λ dia. Cassegrain fed by 20 dB Potter Horn with 0° metal shroud and Sinusoidal Cone radome support Front lobe